MATHEMATICAL ANALYSIS OF ENERGY HARVESTER MODEL

BY

OLEKSANDR VDOVYN

MS, University of New Hampshire, 2015

THESIS

Submitted to the University of New Hampshire

in Partial Fulfillment of

the Requirements for the Degree of

Master of Science

in

Applied Mathematics

September, 2015

This thesis has been examined and approved in partial fulfillment of the requirement for the degree of Master of Science in Applied Mathematics by:

Thesis Director, Marianna Shubov, Professor

Rita Hibschweiler, Professor

Steve Wineberg, Lecturer

On 05/28/2015

Original approval signatures are on file with the University of New Hampshire Graduate School.

TABLE OF CONTENTS

LIST OF TABLES

LIST OF FIGURES

ABSTRACT

MATHEMATICAL ANALYSIS OF ENERGY HARVESTER MODEL

by

Oleksandr Vdovyn

University of New Hampshire, September 2015

Energy Harvesting from ambient waste energy for the purpose of running low-powered electronics has emerged during last decades. The goal of energy harvesting devices is to provide remote sources of electrical power and/or recharge storage devices such as batteries and capacitors. The evolution of low-power-consuming electronics have led to and active academic research in energy harvesting. One of the most studied areas is the use of the piezoelectric effect to convert ambient vibration into useful electrical energy. The focus of this study on placed on detailed mathematical analysis of electromechanical models of piezoelectric energy harvester. The area of vibration-based energy harvesting incorporates knowledge and methods from mechanics, material science, and electrical circuitry. Researches from all three disciplines contribute heavily to energy harvesting literature. The term energy harvester is defined as the generator device undergoing vibrations due to a specific form of excitation. The main focus, therefore, is placed on modeling and electromechanical response of the device for the respective form of excitation rather than investigating the storage components and the power electronics aspects. The electromechanical response of a piezoelectrical energy harvester and the amount of power it generates are completely dependent on the nature

of ambient energy. In the analytical framework of our study, harmonic and non-harmonic forms of ambient excitation can be considered as well as moving-load excitations, periodic inputs and airflow-induced vibrations (aeroelastic energy harvesters). The ultimate goal in this research field is to power small electronic devices by using the vibration energy available in their environment. If this can be achieved, the requirement of an external power source as well as the maintenance costs for periodic battery replacement and the chemical waste of conventional batteries can be significantly reduced.

CHAPTER 1
INTRODUCTION

1.1 Motivation

The history of energy harvesting dates back to the windmill and the waterwheel. People have searched for ways to store the energy from heat and vibrations for many decades. One driving force behind the search for new energy harvesting devices is the desire to power sensor networks and mobile devices without batteries. Energy harvesting is also motivated by a desire to address the issue of climate change and global warming. With the growing threat of pollution, global warming, and energy crises caused by our strong dependence on the dwindling supply of nonrenewable fossil fuels, the search for clean and renewable alternative energy resources is one of the most urgent challenges to the sustainable development of human civilization.

The ultimate goal of energy harvesting is to remove the external power source or battery replacement requirement for small electronic devices. The basic transduction mechanism that can be used to convert the ambient vibration energy to electrical energy is piezoelectric transduction [1].

1.2 Energy Harvesting

Energy harvesting is the process of capturing minute amounts of energy from one or more naturally-occurring energy sources, accumulating them and storing them for later use. In general, energy can be stored in capacitor, super capacitor, or battery. Energy harvesting can be obtained from four main ambient energy sources in our environment: mechanical energy

(vibrations, deformations), thermal energy (temperature gradients or variations), radiant energy (sun, infrared, radio frequency) and chemical energy (chemistry, biochemistry).

A variety of techniques are available for energy harvesting, including piezoelectricity, thermoelectricity, solar and wind powers, ocean waves, physical motions, and etc. [2].

The drastic reduction in power requirements of small electronic components has motivated the research for powering such components by using the vibration energy available in their environment, especially in remote/wireless sensing applications [3]. The idea of vibration-to-electric energy conversion for powering small electronic components by using the ambient vibration energy has been investigated by researches from different disciplines in the last decade.

1.3 Simplified scheme of piezoelectric effect

The main goal of this research is to analyze a mathematical model for electromechanical energy harvester incorporating the idea of piezoelectricity. Below we present schematic picture of piezoelectricity.

A dielectric material is an electrical insulator that can be polarized when an electric field is applied to it. When a dielectric is placed in an electric field, electric charges do not flow through the material as they do in a conductor, but only slightly shift from their average equilibrium positions causing dielectric polarization. Because of dielectric polarization, positive charges are displaced toward the field and negative charges shift in the opposite direction. This creates an internal electric field that reduces the overall field within the dielectric itself [4].

In some crystals polarization can appear without internal field if a crystal is subjected to mechanical deformation. This phenomenon first was observed by Pierre and Jacques Curie in 1880 and called *piezoelectric effect*.

Piezoelectric charge can be seen by covering the edge of crystal wafer by metallic plate.

Lets consider the main properties of piezoelectric crystal on the example of quartz crystal

(SiO_2). Crystals of quartz exist in different crystallographic modifications. The crystals of our interest belong to so called trigonal crystallographic system and usually have the form on the Fig. 1.1. They look like hexagonal prism bounded by two pyramids. Such crystals

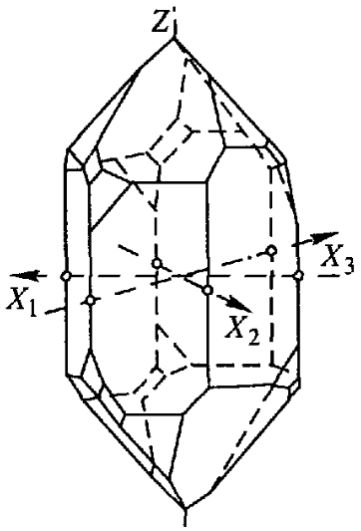

Figure 1.1: Crystal of quartz

are characterized by four crystallographic axes which determine essential directions inside the crystal. One of the axes is $Z-$axis which connects the vertices of pyramid. The three others X_1, X_2 and X_3 are perpendicular to $Z-$axis and connect opposite edges of hexagon prism. The direction Z is piezoelectric non-active (with deformation in Z direction there is no polarization, but with deformation in perpendicular direction to $Z-$axis electrical polarization appears). $Z-$axis is called *optical axis* of the crystal and axes X_1, X_2 and X_3- *electric* or *piezoelectric* axes.

Let us consider the plate of crystal curved perpendicularly in the direction of one of the piezoelectric $X-$axes (Fig. 1.2).

The $Y-$axis is perpendicular to $Z-$axis and $X-$axes. Then with deformation of the plate along axis X on edges $ABCD$ and $EFGH$ opposite polarization charges appear. Such piezoelectric effect called *longitudinal*. Piezoelectric effect which can be seen by the deformation in the direction along $Y-$axis (with polarization charges on edges $ABCD$ and $EFGH$) is called *transverse* piezoelectric effect. Piezoelectric effect can be explained by ion structure

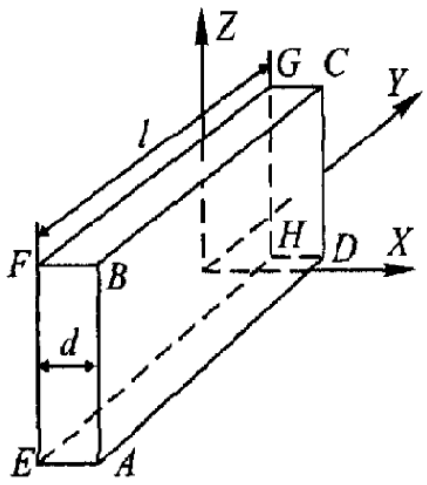

Figure 1.2: Plate of quartz crystal curved perpendicularly to one of the X axes

in quartz crystals (Fig. 1.3).

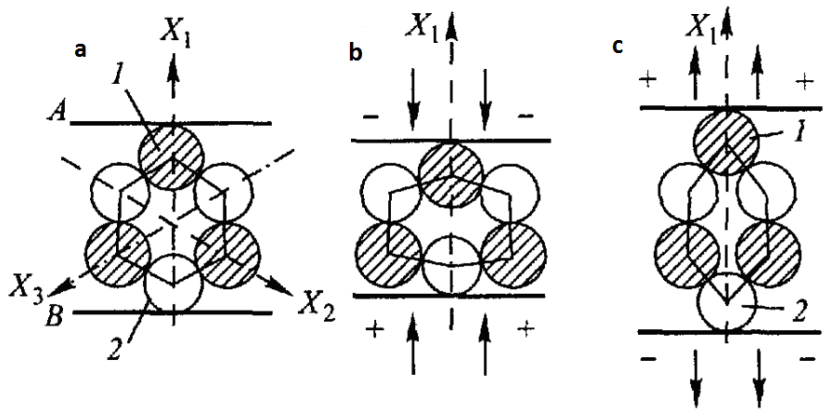

Figure 1.3: Projection of quartz crystal. Configuration of ions

With deformation of crystal, the positive and negative grids are shifted with respect to each other, and therefore the electrical moment is changed. With the change of electrical moment piezoelectric effect appears. On Fig.1.3 the projection of positive ions Si (shaded circles) and negative ions O (white circles) lie on the plane perpendicular to $Z-$axis. This picture is not actual representation of ion configuration (the ions dont lie on the same plane, the number of ions is greater than on the picture), but the symmetry of positional relationship can clearly describe the property of ions. Fig.1.3 (a) corresponds to an undeformed

crystal. With deformation (compression) along X_1-axis low-level cell is deformed (Fig.1.3 (b)). Positive ion 1 and negative ion 2 are 'pushed' inside of the cell, and the charge on the edges A and B become smaller, or its equivalent to appearance negative charge on the edge A and positive charge on the edge B. With deformation (stretching) along X_1-axis (Fig.1.3 (c)) the situation is the opposite: ions 1 and 2 are 'pushed' out of the cell. Therefore on the edge A additional positive charge appears, and on the edge $B-$ negative charge. The analysis of symmetry in the theory of solid material shows that piezoelectric effect can be seen only in the crystals where low-level cell doesn't have the center of symmetry [5]. The positional relationship of ions in the cell of quartz is such that there is no center symmetry, and therefore piezoelectric effect can be seen. Out of 32 crystallographic classes of symmetry, 21 classes dont have the center of symmetry, but one of them is piezoelectric non-active. Therefore crystals of 20 classed considered to be piezoelectric.

1.4 Vibration-to-electric energy harvesting mechanisms

There are three basic vibration-to-electric energy conversion mechanisms proposed by Williams and Yates [6], they are electromagnetic, electrostatic and piezoelectric transduction.

The principle for electromagnetic conversion is based on idea of electromagnetic induction discovered by Faraday in 1831. Electromagnetic induction is a process where a conductor

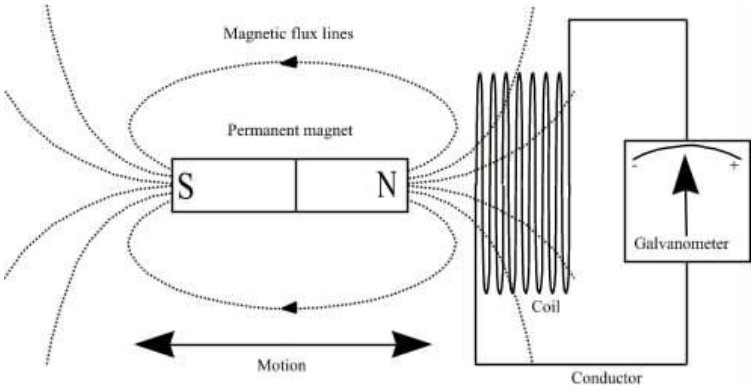

Figure 1.4: Basic principle of electromagnetic induction

placed in a changing magnetic field (or a conductor moving through a stationary magnetic

field) causes the production of a voltage across the conductor. This process of electromagnetic induction, in turn, causes an electrical current - it is said to induce the current.

The most common application has been the bicycle dynamo (or alternator, more correctly, as these devices generate alternating current). Although inefficient, this has been a reliable, easy to manufacture device that has kept bicycle lights going in the night for decades.

The Seiko Kinetic watches are another good example of using the principle of generating energy from movement in a small scale, with a storage device such as a rechargeable battery or a capacitor, used side by side with the generator, in order to store electrical energy for later use.

A piezoelectric material will produce an electric field and consequently a voltage when deformed under an applied stress. The principle of piezoelectric energy harvesting will be explained in the next section.

A summary of advantages and drawbacks of electromagnetic, electrostatic and piezoelectric devices is presented in Table 1.1. In most cases, piezoelectric and electrostatic devices are more appropriate for small scale energy harvesters ($< 1 - 10cm^3$) while electromagnetic converters are better for larger devices [7]. Among these transduction mechanisms, piezo-

	Piezoelectric devices	Electromagnetic devices	Electrostatic devices
Advantages	• High output voltages • High capacitance • Ability to be manufactured in any shape and size	• High output currents • Long lifetime proven • Robustness	• High output voltages • Possibility to build low-cost systems • Coupling coefficient easy to adjust • High coupling coefficients reachable • Size reduction increases capacitance
Drawbacks	• Expensive (material) • Coupling coefficient linked to material properties	• Low output voltages • Hard to develop MEMS devices • May be expensive (material) • Low efficiency in low frequencies and small sizes	• Low capacitance • High impact of parasitic capacitances • Need to control μm dimensions • No direct mechanical-to-electrical conversion for electret-free converters

Table 1.1: Advantages and drawbacks of converters.

electric transduction has received the greatest attention in the last few years, and the main

concentration of this work is mathematical model of piezoelectric energy harvester.

1.5 Piezoelectric Energy Harvesting

Materials which generate an electric potential in response to mechanical stress are considered to be piezoelectric materials. Such materials will also change shape when an electric field is applied to them.

The process of generation of an electric charge when piezoelectric materials subjected to mechanical stresses is called piezoelectric effect.

A typical piezoelectric energy harvester is in the form of the cantilevered beam with one or two piezoceramic layers (a unimorph or a bimorph) [8]. We use the Euler-Bernoulli model to describe the transverse vibrations of the beam. The unimorph cantilever with a piezoceramic layer connected to a resistive load is presented on Fig. 1.5. The harvester beam is located on

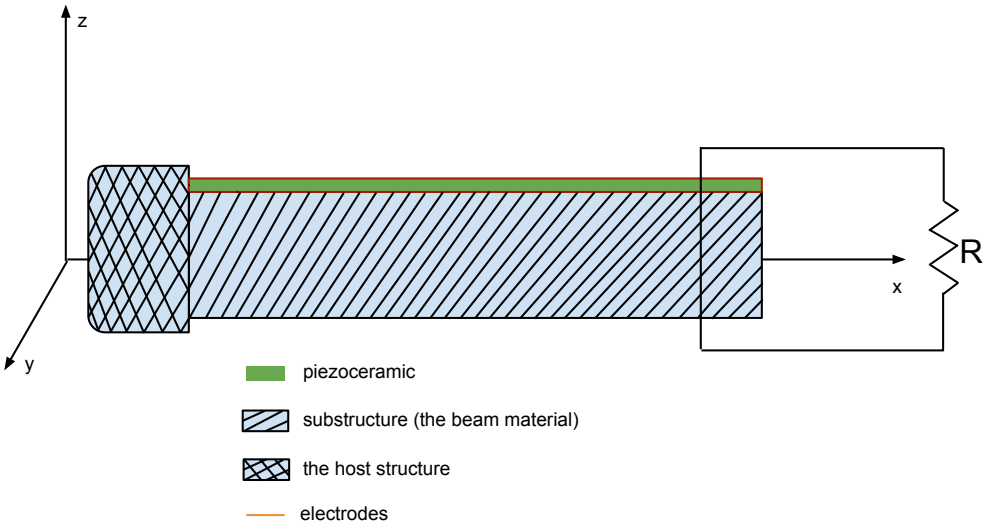

Figure 1.5: Unimorph cantilever with a piezoceramic layer connected to a resistive load.

a vibrating host structure and the dynamic strain induced in the piezoceramic layer results in an alternating voltage output across their electrodes. A pair of electrodes is covering the top and the bottom faces of the piezoceramic layer. The electrodes are connected to a resistive load. The load is considered in an electrical circuit along with the internal capacitance of

the piezoceramic layer, which is assumed to be a perfect insulator. If the beam vibrates due to some external load then a dynamic strain appears in the piezoceramic layer. Due to the piezoelectric effect this strain results in an alternating voltage output across the electrodes. This output can be harvested for charging batteries of running low- powered electronic devices.

CHAPTER 2
PHYSICAL MODELING IN MATHEMATICAL STATEMENT OF THE PROBLEM

2.1 Physical model of piezoelectric energy harvester

We consider a piezoelectric energy harvester in the form of cantilever (clamped-free) beam with a piezoceramic layer attached to the upper face of a beam. The beam is assumed to be thin. We use the Euler - Bernoulli model to describe the transverse vibrations of the beam. A pair of electrodes is covering the top and the bottom faces of the piezoceramic layer. The electrodes are assumed to be perfectly conductive. The electrodes are connected to a resistive load. The load is considered in an electrical circuit along with the internal capacitance of the piezoceramic layer, which is assumed to be a perfect insulator. If the beam vibrates due to some external load, then a dynamic strain appears in the piezoceramic layer. Due to the piezoelectric effect this strain results in an altenating voltage output across the electrodes. This output can be harvested for charging batteries of running low- powered electronic devices.

On the other hand, the electric potential difference between the electrodes generates an electric field in the piezoceramic layer. This electric field produces a stress on the piezoceramic due to *the converse piezoelectric effect*. So, the dynamics of the beam is affected by the electric circuit. As a result, the energy harvester is modeled by a coupled system of two differential equations. The first of them is a hyperbolic partial differential equation for the Euler-Bernoulli beam that contains an additional term depending on the voltage on the electrodes. This term represents *the converse piezoelectric effect*. In other words, *the*

backward piezoelectric coupling effect modifies the vibration response of the cantilever. The second equation is just the Kirchhoff's law for the electric circuit. This equation is a linear first order ordinary differential equation with respect to the voltage across the electrodes. The equation contains an additional integral term depending on the transverse displacement of the beam. This term represents *the direct piezoelectric effect*.

Remark 2.1. 1) In practical applications the beam may be located on a vibrating host structure. Alternatively, the vibration of the beam may be due to an ambient airflow. We describe below just the equations that govern the model without the external load term that generates the vibrations.

2) We consider a harvester with a single piezoceramic layer (a unimorph configuration). In practical applications most of piezoelectric energy harvesters have two piezoceramic layers (bimorph configuration). These layers can be connected to a resistive load either in a series or in a parallel manner. However, the equations of the model are the same for unimorph and for bimorph configurations, for series or parallel connection. The only differences are in the values of the parameters entering these equations. So, we consider the electromechanical model with the simplest electric circuit.

Now we formulate an initial boundary value problem for a model of unimorph piezoelectric harvester. Assume that piezoceramic layer is attached to Euler-Bernoulli beam of a finite length L, $0 < L < \infty$. Let $w(x,t)$ be a transverse displacement of a beam at a position x and time moment t, $0 \le x \le L,\ t \ge 0$. Let $v(t)$ be output voltage across the electrodes of the piezoceramic layer. Then the following linear system of coupled differential equations is valid for the unknown w and v [9]:

$$m\frac{\partial^2 w(x,t)}{\partial t^2} + c_s I\frac{\partial^5 w(x,t)}{\partial x^4 \partial t} + c_a\frac{\partial w(x,t)}{\partial t} + YI\frac{\partial^4 w(x,t)}{\partial x^4} - \theta v(t)\left\{\delta'(x) - \delta'(x-L)\right\} = 0, \quad (2.1)$$

$$C\frac{dv(t)}{dt} + \frac{1}{R}v(t) + \kappa\int_0^L \frac{\partial^3 w(x,t)}{\partial^2 x \partial t}dx = 0, \quad (2.2)$$

$$w(0,t)=0, \quad \left.\frac{\partial w(x,t)}{\partial x}\right|_{x=0}=0, \tag{2.3}$$

$$\left[YI\frac{\partial^2 w(x,t)}{\partial x^2}+c_sI\frac{\partial^3 w(x,t)}{\partial x^2\partial t}\right]_{x=L}=0, \qquad \left[YI\frac{\partial^3 w(x,t)}{\partial x^3}+c_sI\frac{\partial^4 w(x,t)}{\partial x^3\partial t}\right]_{x=L}=0; \tag{2.4}$$

$$w(x,t)=w_0(x), \quad \left.\frac{\partial w(x,t)}{\partial t}\right|_{t=0}=w_1(x), \quad v(0)=v_0. \tag{2.5}$$

The following notations have been used in the structural Eq.(2.1): m-density of a beam (mass per unit length), c_a-viscous air damping coefficient, c_s- Kelvin-Voigt (strain-rate) damping coefficient, $Y-$the Young modulus, $I-$cross section moment of inertia with respect to the neutral axis ($YI-$ the bending stiffness), $\theta-$converse piezoelectric effect backward coupling coefficient, $\delta-$ is the Dirac delta function, whose derivative δ' should be understood in a distributional sense.

The following notations have been used in the electrical circuit equation for the thin piezoceramic layer attached to the beam: $C-$internal capacitance of the piezoceramic layer, $R-$resistance of the external load, $\kappa-$direct piezoelectric effect coupling coefficient.

Regarding boundary conditions, we assume that the beam is clamped at the left end $x=0$ (see (2.3)) and the right end of the beam is free (see (2.4)). We impose the initial state (2.5) in a standard fashion. In the next two sections we briefly outline the origin of mechanical and electric circuit equations.

2.2 Origin of equation of motion for free vibrations of beam

As is known, the equation of motion for the transverse vibrations of a thin beam $w(x,t)$ has the form [10]:

$$m\frac{\partial^2 w(x,t)}{\partial t^2}=T\frac{\partial^2 w(x,t)}{\partial x^2}+\frac{\partial N(x,t)}{\partial x}, \tag{2.6}$$

where m is mass per unit length, T-internal tension (we will assume $T = 0$), $N(x,t)$- the shear force.

Remark 2.2. For brevity we did not include into (2.6) the Kelvin-Voigt (strain-rate) and viscous air (external) damping terms that are present in (2.1). These terms can be easily added to the left-hand side of (2.6).

Let $M(x,t)$ be the internal bending moment about the y- axis. Conservation of the angular momentum implies [11]

$$N(x,t) = \frac{\partial M(x,t)}{\partial x}. \tag{2.7}$$

The following constitutive relation holds:

$$M(x,t) = -YI\frac{\partial^2 w(x,t)}{\partial x^2}, \tag{2.8}$$

which means that M is proportional to the curvature of the beam, which for small displacements is equal to $\frac{\partial^2 w}{\partial x^2}$. The proportionality coefficient's is the bending stiffness. In (2.8) we use the standard sign agreement: positive bending moment creates a negative curvature.

Substituting (2.7), (2.8) into (2.6) and taking $T = 0$ we get the classical Euler-Bernoulli equation for vibration of a thin beam:

$$m\,\frac{\partial^2 w(x,t)}{\partial t^2} + YI\,\frac{\partial^4 w}{\partial x^4} = 0. \tag{2.9}$$

In the case of a beam with attached piezoceramic layer the constitutive relation between the displacement and the internal bending moment (see (2.8)) contains an additional term:

$$M(x,t) = -YI\,\frac{\partial^2 w(x,t)}{\partial x^2} + \theta v(t)\left\{H(x) - H(x-L)\right\}. \tag{2.10}$$

Here $v(t)$- voltage across the electrodes of the piezoceramic layer, θ-backward coupling coefficient, $H(x)$- Heaviside step function. The second term in the right-hand side of (2.10) is

due to the converse piezoelectric effect. Namely, the voltage $v(t)$ produces a uniform electric field $E = -\frac{v(t)}{h}$ (h- the thickness of the layer) in the piezoceramic layer. Due to the converse piezoelectric effect, this field generates an additional bending moment that is constant along the beam ($0 \leq x \leq L$). The additional term is multiplied by the characteristic function of the interval $[0, L]$: $\chi(x) = H(x) - H(x - L)$.

Replacing constitutive relation (2.8) by (2.10), combining with (2.7) and substituting into equation of motion (2.6) (and taking into account $H'(x) = \delta(x)$) we arrive at the equation of motion (2.1) without the damping terms (as pointed out in Remark above, to get these terms we should include them into (2.6) from the very beginning).

2.3 Origin of electrical circuit equation

The piezoelectric element from Fig.1.5 is represented as a current source $i_p(t)$ in parallel its internal capacitance C connected to external load R. In the sequel, we use the following

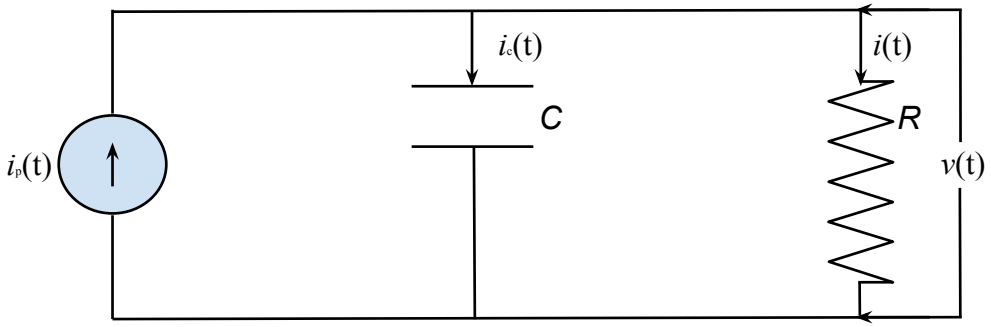

Figure 2.1: Electrical circuit of the harvester presented on Fig. 1.5

notations: $R-$ resistance of the external load, $v(t)-$ output voltage, $C-$ internal capacitance of the piezoelectric layer, $i_p(t)-$ alternating current across the piezoceramic layer, $i_c(t)-$ alternating current across the capacitor, $i(t)-$ total current across the external resistive load. If we use the directions of the currents shown on Fig. 2.1, the Kirchhoff's law for the electrical circuit has the form

$$i_c(t) + i(t) - i_p(t) = 0. \tag{2.11}$$

Now we derive Eq.(2.2) from the Kirchhoff's law (2.11). To this end, we present formulas for all three terms in (2.11).

a) The charge of the capacitor C is given by

$$q(t) = C\, v(t), \tag{2.12}$$

which yields the current across the capacitor as

$$i_C(t) = \frac{dq(t)}{dt} = C\, \frac{dv(t)}{dt}. \tag{2.13}$$

(Sign "plus" in (2.13) is due to the current direction shown in Fig.1.2).

b) According to the Ohm's law, the current through the resistive load, R, is given by

$$i(t) = \frac{1}{R}\, v(t). \tag{2.14}$$

c) To justify the formula for $i_p(t)$, we need some additional notations: $h-$ thickness of the piezoelectric layer (in $z-$ direction), $b-$ width of the piezoelectric layer (in $y-$ direction), $A = bL-$ area of the top face of the beam and of each of the electrodes, h_1- distance from the neutral axis of the beam (the $x-$ axis) to the centerline of the piezoceramic layer; $D(x, z, t)-$ electric displacement (directed along $z-$ axis) inside the piezoelectric layer, $E(t)-$ electric field inside the piezoceramic layer; $S(x, z, t)-$ the strain at level z from the neutral axis produced by the displacement of the beam, $d-$ the piezoelectric constant (of the direct piezoelectric effect), $\varepsilon-$ the permittivity of the piezoceramic material.

We have the following relations.

(i) According to a well known elementary formula for the capacitance of a flat capacitor [12]

$$C = \frac{\varepsilon A}{h} = \frac{\varepsilon bL}{h}. \tag{2.15}$$

(ii) The electric field

$$E(t) = -\frac{v(t)}{h}. \tag{2.16}$$

(iii) Strain inside the piezoelectric layer and the beam is proportional to the curvature of the beam:

$$S(x, z, t) = -z\,\frac{\partial^2 w(x,t)}{\partial x^2}. \tag{2.17}$$

(Here we use the sign agreement mentioned above: a positive bending creates a negative curvature.)

(iv) The constitutive relation between D, S, and E due to the direct piezoelectric effect has the form [13]

$$D(x, z, t) = d\,S(x, z, t) + \varepsilon\,E(t). \tag{2.18}$$

(v) Substituting (2.16), (2.17) into (2.18) we obtain

$$D(x, z, t) = -dz\,\frac{\partial^2 w(x,t)}{\partial x^2} - \frac{\varepsilon}{h}\,v(t). \tag{2.19}$$

(vi) According to the Gauss's [14] law, the total charge on the electrodes attached to the top and bottom faces of the piezoceramic layer is

$$Q(t) = \int_A D(x, h, t)dA = \int_0^L \int_0^b D(x, h, t)dydx = b\int_0^L D(x, h, t)dx. \tag{2.20}$$

(vii) Substituting (2.19) with $z = h_1$ into (2.20) we get

$$Q(t) = -bdh_1 \int_0^L \frac{\partial^2 w(x,t)}{\partial x^2}dx - \frac{\varepsilon bL}{h}v(t). \tag{2.21}$$

(viii) Now we have an alternative formula for the total current across the resistive load

$$i(t) = \frac{dQ(t)}{dt} = -\kappa \int_0^L \frac{\partial^3 w(x,t)}{\partial^2 x \partial t}dt - C\,\frac{dv(t)}{dt}, \tag{2.22}$$

where we denoted $\kappa = bdh_1$ and have taken into account (2.15).

(ix) Now we substitute (2.22) and (2.13) into (2.11) to get

$$i_p(t) = i(t) + i_C(t) = -\kappa \int_0^L \frac{\partial^3 w(x,t)}{\partial^2 x\, \partial t} dx. \tag{2.23}$$

It remains to notice that substitution of (2.13), (2.14), and (2.23) into (2.11) gives exactly Eq.(2.2).

2.4 Equivalent formulation of the initial boundary-value problem

Below we represent an equivalent formulation of the initial boundary-value problem.

Lemma 2.2. *Initial boundary-value problem* (2.1)− (2.4) *is equivalent to the following problem:*

$$m\,\frac{\partial^2 w(x,t)}{\partial t^2} + c_s\, I \frac{\partial^5 w(x,t)}{\partial x^4 \partial t} + c_a\,\frac{\partial w(x,t)}{\partial t} + Y I\,\frac{\partial^4 w(x,t)}{\partial x^4} = 0, \tag{2.24}$$

$$C\,\frac{dv(t)}{dt} + \frac{1}{R}\,v(t) + \kappa \int_0^L \frac{\partial^3 w(x,t)}{\partial^2 x\, \partial t} dx = 0, \tag{2.25}$$

$$w(0,t) = 0, \quad \frac{\partial w}{\partial x}(0,t) = 0, \tag{2.26}$$

$$\left[Y I \frac{\partial^2 w}{\partial x^2} + c_s I \frac{\partial^3 w}{\partial x^2 \partial t} \right]_{x=L} = \theta v(t), \tag{2.27}$$

$$\left[Y I \frac{\partial^3 w}{\partial x^3} + c_s I \frac{\partial^4 w}{\partial x^3 \partial t} \right]_{x=L} = 0. \tag{2.28}$$

Notice, the only difference between (2.1)− (2.4) and (2.24)− (2.28) is that the distributional term $\theta v(t)[\delta'(x) - \delta'(x-L)]$ in (2.1) is replaced by additional term $\theta v(t)$ in the right-hand

side of boundary condition (2.27). The standard initial conditions for both problems have the form:

$$w(x,0) = w_0(x),\ \frac{\partial w}{\partial t}(x,0) = w_1(x),\ x \in [0,L].$$

Proof of Lemma 2.2. To show that problems (2.1)– (2.4) and (2.24)– (2.28) are equivalent we check that their weak (variational) formulations coincide. Let $\mathcal{P} = \{\varphi \in C^\infty[0,L] : \varphi(0) = \varphi'(0) = 0\}$ be the class of test functions. Let us multiply both equations (2.1) and (2.24) by $\varphi \in \mathcal{P}$ and integrate over $[0,L]$. Integrating by parts twice in the second and forth terms of (2.1) and (2.24) and taking into account the distributional terms in (2.1) we arrive at the same variational (weak) formulations of both problems:

$$\begin{aligned} &\int_0^L \left(m\frac{\partial^2 w(x,t)}{\partial t^2} + c_a \frac{\partial w(x,t)}{\partial t} \right) \varphi(x) dx \\ &+ \int_0^L \left(c_s I \frac{\partial^3 w(x,t)}{\partial x^2 \partial t} + \frac{\partial^2 w(x,t)}{\partial x^2} \right) \varphi''(x) dx - \theta v(t) \varphi'(L) = 0 \end{aligned} \tag{2.29}$$

for any $\varphi \in \mathcal{P}$. In addition to (2.29) we assume that w satisfies boundary conditions (2.26).

The lemma is shown. ■

In what follows we assume that the damping coefficient are such that $c_a > 0$ and $c_s = 0$. In this case we have

$$m\frac{\partial^2 w(x,t)}{\partial t^2} + c_a \frac{\partial w(x,t)}{\partial t} + YI\frac{\partial^4 w(x,t)}{\partial x^4} = 0, \tag{2.30}$$

$$C\frac{dv(t)}{dt} + \frac{1}{R}v(t) + \kappa \int_0^L \frac{\partial^3 w(x,t)}{\partial^2 x \partial t} dx = 0, \tag{2.31}$$

$$w(0,t) = 0, \quad \frac{\partial w}{\partial x}(0,t) = 0, \tag{2.32}$$

$$YI\frac{\partial^2 w}{\partial x^2}(L,t) = \theta v(t), \tag{2.33}$$

$$\frac{\partial^3 w}{\partial x^3}(L,t) = 0. \tag{2.34}$$

The integral term in (2.31) can be simplified by taking into account the second condition (2.32), i.e.,

$$\int_0^L \frac{\partial^3 w(x,t)}{\partial^2 x \partial t} dx = \frac{\partial}{\partial t}\frac{\partial w}{\partial x}(L,t). \tag{2.35}$$

2.5 First approach to the solution of the initial boundary-value problem

Let us consider Eq.(2.31) that satisfies an initial condition $v(0) = v_0$. Solving this initial value problem, we get

$$v(t) = -\frac{\kappa}{C}\int_0^t e^{-\frac{1}{CR}(t-\tau)}\frac{\partial}{\partial \tau}\frac{\partial w}{\partial x}(L,\tau)d\tau + v_0. \tag{2.36}$$

Integrating by parts in (2.36) we reduce the expression for $v(t)$ to:

$$v(t) = -\frac{\kappa}{C}\left[\frac{\partial w}{\partial x}(L,t) - e^{-\frac{1}{CR}t}\frac{\partial w}{\partial x}(L,0) - \frac{1}{CR}\int_0^t e^{-\frac{1}{CR}(t-\tau)}\frac{\partial w}{\partial x}(L,\tau)d\tau\right] + v_0. \tag{2.37}$$

Using (2.37) we obtain the following initial boundary-value problem for the structural component $w(x,t)$:

$$m\frac{\partial^2 w}{\partial t^2} + c_a\frac{\partial w}{\partial t} + YI\frac{\partial^4 w}{\partial x^4} = 0, \tag{2.38}$$

Boundary conditions:

$$w(0,t) = 0, \quad \frac{\partial w}{\partial x}(0,t) = 0; \tag{2.39}$$

$$\begin{aligned} YI\frac{\partial^2 w}{\partial x^2}(L,t) = \theta - \frac{\kappa}{C}\Bigg[&\frac{\partial w}{\partial x}(L,t) - e^{-\frac{1}{CR}t}\frac{\partial w}{\partial x}(L,0) \\ &-\frac{1}{CR}\int_0^L e^{-\frac{1}{CR}(t-\tau)}\frac{\partial w}{\partial x}(L,\tau)d\tau\Bigg] + v_0, \end{aligned} \tag{2.40}$$

$$YI\frac{\partial^3 w}{\partial x^3}(L,t) = 0. \tag{2.41}$$

$$w(x,0) = w_0(x), \quad \frac{\partial w}{\partial t}(x,0) = w_1(x). \tag{2.42}$$

Due to presence of the Volterra integral operator in the right-hand side of condition (2.40), it is natural to rewrite the problem in terms of the Laplace transformation of w. Let $W(\lambda, t)$ be defined as

$$W(x,\lambda) = \int_0^\infty w(x,t)e^{-\lambda t}dt, \quad \lambda \in \mathbb{C}. \tag{2.43}$$

1. Equation (2.38) become

$$\lambda^2 W(x,\lambda) + \lambda c_a W(x,\lambda) + \frac{YI}{m}\ \frac{\partial^4 W(x,\lambda)}{\partial x^4} - \lambda w_0(x) - w_1(x) = 0. \tag{2.44}$$

2. Boundary conditions:

   (a) $x = 0$:

$$W(0,\lambda) = 0, \quad \frac{\partial W}{\partial x}(0,\lambda) = 0; \tag{2.45}$$

   (b) $x = L$:

$$YI\frac{\partial^2 W(L,\lambda)}{\partial x^2} = \theta V(\lambda), \tag{2.46}$$

$$\frac{\partial^3 W(L,\lambda)}{\partial x^3} = 0. \tag{2.47}$$

3. Expression for $V(\lambda)$:

$$
\begin{aligned}
V(\lambda) &= -\frac{\kappa}{C}\mathcal{L}\left\{e^{-\frac{1}{CR}t}\right\}\mathcal{L}\left\{\frac{\partial}{\partial t}\frac{\partial w}{\partial x}(L,t)\right\} + \mathcal{L}\{v_0\} \\
&= -\frac{\kappa}{C}\frac{1}{\lambda+\frac{1}{CR}}\left[\lambda\frac{\partial W}{\partial x}(L,t) - \frac{\partial w}{\partial x}(L,0)\right] + \frac{v_0}{\lambda} \\
&= -\frac{\kappa}{C}\frac{1}{\lambda+\frac{1}{CR}}\left[\lambda\frac{\partial W}{\partial x}(L,t) - \frac{\partial w_0}{\partial x}(L)\right] + \frac{v_0}{\lambda}.
\end{aligned} \tag{2.48}
$$

Now let us rewrite (2.44) − (2.48) for the case of zero initial conditions

$w_0 = 0,\ w_1(x) = 0,\ v_0 = 0.$

1. Equation:

$$
\lambda^2 W(x,\lambda) + \lambda c_a W(x,\lambda) + \frac{YI}{m}\frac{\partial^4 W(x,\lambda)}{\partial x^4} = 0. \tag{2.49}
$$

2. Boundary conditions:

(a) $x = 0$:

$$
W(0,\lambda) = 0, \quad \frac{\partial W}{\partial x}(0,\lambda) = 0; \tag{2.50}
$$

(b) $x = L$:

$$
\frac{CYI}{\kappa\theta}\frac{\partial^2 W}{\partial x^2}(L,\lambda) = -\frac{\lambda}{\lambda+\frac{1}{CR}}\frac{\partial W}{\partial x}(L,\lambda), \tag{2.51}
$$

$$
\frac{\partial^3 W}{\partial x^3}(L,\lambda) = 0. \tag{2.52}
$$

Remark 2.3 Even if we succeed in finding an explicit formula for the solution of the problem (2.49) − (2.52), it is an extremely difficult problem to write space-time representation for the beam displacement and the voltage. So in what follows we suggest an alternative method of solution.

CHAPTER 3

OPERATOR FORMULATION OF INITIAL-BOUNDARY PROBLEM. SPECTRAL PROPETRIES OF DYNAMICS GENERATOR

3.1 Statement of the problem

Equation of motion for the free vibrations of the beam:

$$m\frac{\partial^2 w(x,t)}{\partial t^2} + c_s I\frac{\partial^5 w(x,t)}{\partial x^4 \partial t} + c_a\frac{\partial w(x,t)}{\partial t} + YI\frac{\partial^4 w(x,t)}{\partial x^4} = 0. \tag{3.1}$$

Electrical circuit equation for the thin piezoceramic layer attached to the beam:

$$C\frac{dv(t)}{dt} + \frac{1}{R}v(t) + \kappa\int_0^L \frac{\partial^3 w}{\partial^2 x \partial t}dx = 0. \tag{3.2}$$

For the present paper, we assume that the internal damping (the Kelvin-Voight damping) is small enough to be neglected, i.e., let $c_s = 0$. It is convenient to use scaled physical quantities with the new set of notations.

Letting

$$G = \frac{c_a}{m}, \qquad E = \frac{YI}{m}, \qquad H = \frac{1}{CR}, \qquad h = \frac{\kappa}{C}, \qquad \Theta = \frac{\theta}{m}, \tag{3.3}$$

we rewrite the boundary-value problem as follows:

$$\frac{\partial^2 w(x,t)}{\partial t^2} + G\frac{\partial w(x,t)}{\partial t} + E\frac{\partial^4 w(x,t)}{\partial x^4} = 0, \tag{3.4}$$

$$\frac{\partial v(t)}{\partial t} + Hv(t) + h\left\{ \left.\frac{\partial^2 w(x,t)}{\partial x \partial t}\right|_{x=L} - \left.\frac{\partial^2 w(x,t)}{\partial x \partial t}\right|_{x=0} \right\} = 0, \tag{3.5}$$

$$w(0,t) = \left.\frac{\partial w(x,t)}{\partial x}\right|_{x=0} = 0, \tag{3.6}$$

$$E \left.\frac{\partial^2 w(x,t)}{\partial x^2}\right|_{x=L} = \Theta v(t), \quad \left.\frac{\partial^3 w(x,t)}{\partial x^3}\right|_{x=L} = 0. \tag{3.7}$$

Definition 1.1. Let $A \cdot |_a$ be a differential operation defined on a smooth function f by the rule

$$A \cdot |_a [f] = \left.\frac{df}{dx}\right|_{x=a} = f'(a). \tag{3.8}$$

Now let $(w(x,t),\ v(t))$ be a solution of the above system. Introduce a three – component vector

$$U(x,t) = \left(w(x,t), \dot{w}(x,t), v(t)\right)^T, \tag{3.9}$$

where the superscript "T" means transposition. Direct verification shows that system (3.4) – (3.7) can be written in the form:

$$\frac{d}{dt}\left(\mathbb{A}U\right)(x,t) = \left(\mathbb{B}U\right)(x,t), \qquad U(x,0) = U_0(x), \qquad U_0(x) = \left(w_0(x), w_1(x), v_0\right)^T. \tag{3.10}$$

where

$$\mathbb{A} = \begin{bmatrix} 1 & 0 & 0 \\ G & 1 & 0 \\ h\left[A \cdot |_L - A \cdot |_0\right] & 0 & 1 \end{bmatrix}, \tag{3.11}$$

$$\mathbb{B} = \begin{bmatrix} 0 & 1 & 0 \\ -E\frac{d^4}{dx^4} & 0 & 0 \\ 0 & 0 & -H \end{bmatrix}. \tag{3.12}$$

Eq. (3.10) will be considered on functions satisfying the boundary conditions

$$\begin{aligned} &w(0,t) = w'(0,t) = w'''(L,t) = 0, \\ &Ew''(L,t) = \Theta v(t). \end{aligned} \tag{3.13}$$

Let us fix t in (3.9) and consider a three – component vector function of x. Without misunderstanding we use the same notation U, i.e.,

$$U(x) = (u_0(x), u_1(x), u_2)^T .$$

Energy space. Our goal is to rewrite the initial boundary-value problem as the first order in time evolution in a Hilbert space

$$\mathcal{H} = H_0^2 \times L^2 \times \mathbb{C}. \tag{3.14}$$

Let $\mathcal{H}$ be a closure of smooth functions, such that $u_0(0) = u_0'(0) = 0$ in the norm

$$\|U\|_{\mathcal{H}}^2 = \frac{1}{2}\left[\int_0^L \left(E|u_0''(x)|^2 + |u_1(x)|^2\right) dx + |u_2|^2\right]. \tag{3.15}$$

Our first result is the following lemma.

Lemma 3.2. *A linear operator in $\mathcal{H}$ defined by formula* (3.11) *is bounded with bounded inverse.*

Proof. Let $V(x) = (\mathbb{A}U)(x)$. To prove that $\mathbb{A}$ is a bounded operator in $\mathcal{H}$, one has to show that there exists an absolute constant C_0 such that

$$\|\mathbb{A}U\|_{\mathcal{H}} \le C_0 \|U\|_{\mathcal{H}}, \quad U \in \mathcal{H}. \tag{3.16}$$

Let us estimate $\|V\|_{\mathcal{H}}$ where

$$V(x) = (\mathbb{A}U)(x) = (u_0(x),\ Gu_0(x) + u_1(x),\ h(u_0'(L) - u_0'(0)) + Hu_2)^T. \tag{3.17}$$

Using formula (3.15) we have

$$2\|V\|_{\mathcal{H}}^2 = \int_0^L E|u_0''(x)|^2 dx + \int_0^L |Gu_0(x) + u_1(x)|^2 dx + h^2|u_0'(L) - u_0'(0) + u_2|^2. \tag{3.18}$$

It can be readily seen that with some absolute constant $\widehat{C_0}$ the following estimate holds:

$$\int_0^L |Gu_0(x) + u_1(x)|^2 dx \le \widehat{C_0} \left\{ \int_0^L |u_0(x)|^2 dx + \int_0^L |u_1(x)|^2 dx \right\}. \tag{3.19}$$

To modify (3.19), we note that due to $u_0(0) = u_0'(0)$, we have $u_0(x) = \int_0^x d\xi \int_0^\xi u_0''(\eta) d\eta$. Thus

$$\begin{aligned} |u_0(x)| &\le \int_0^x d\xi \sqrt{\int_0^\xi d\xi} \sqrt{\int_0^\xi |u_0''(\eta)|^2 d\eta} = \int_0^x d\xi \sqrt{\xi} \sqrt{\int_0^\xi |u_0''(\eta)|^2 d\eta} \\ &\le \sqrt{L} \int_0^x d\xi \sqrt{\int_0^\xi |u_0''(\eta)|^2 d\eta} \le \sqrt{L} \int_0^L d\xi \sqrt{\int_0^\xi |u_0''(\eta)|^2 d\eta} \\ &\le \sqrt{L} \int_0^L d\xi \sqrt{\int_0^L |u_0''(\eta)|^2 d\eta} = L\sqrt{L} \sqrt{\int_0^L |u_0''(\eta)|^2 d\eta} \end{aligned} \tag{3.20}$$

From (3.20), it follows that

$$\int_0^L |u_0(x)|^2 dx \le L^4 \int_0^L |u_0''(x)|^2 dx \tag{3.21}$$

Combining (3.19) and (3.21), we obtain

$$\int_0^L |Gu_0(x) + u_1(x)|^2 dx \le C_1 \left\{ \int_0^L |u_0''(x)|^2 dx + \int_0^L |u_1(x)|^2 dx \right\}, \tag{3.22}$$

where C_1 is an absolute constant. Now we consider $|u_0'(L) - u_0'(0) + Hu_2|^2 = |u_0'(L) + Hu_2|$

and have

$$|u_0'(L) - u_0'(0) + Hu_2|^2 = |u_0'(L) + Hu_2|^2 \leq C_2 \left\{|u_0'(L)|^2 + H^2|u_2|^2\right\}. \tag{3.23}$$

Notice

$$|u_0'(L)|^2 = \left|\int_0^L u_0''(\xi)d\xi\right| \leq \int_0^L d\xi \int_0^L |u_0''(\xi)|^2 d\xi = L\int_0^L |u_0''(\xi)|^2 d\xi. \tag{3.24}$$

Collecting together (3.22), (3.23) and (3.24), we obtain that there exists $C_0 > 0$ such that

$$\|V\|_{\mathcal{H}} \leq C_0 \|U\|_{\mathcal{H}}$$

which means that $\mathbb{A} \in \Re(\mathcal{H})$, where $\Re(\mathcal{H})$ is the set of all bounded operators on $\mathcal{H}$.

To show that $\mathbb{A}^{-1} \in \Re(\mathcal{H})$, we start with the derivation of a formula for $\mathbb{A}^{-1}$. To this end, consider the following equation

$$\mathbb{A}F = \mathbb{G}, \tag{3.25}$$

where $\mathbb{G}$ is an arbitrary vector from $\mathcal{H}$. If $\mathbb{G}(x) = (g_0(x), g_1(x), g_2)^T \in \mathcal{H}$, then equation (3.25) yields the following system of equations for unknown components of vector $F = (f_0, f_1, f_2)$

$$f_0(x) = g_0(x), \tag{3.26}$$

$$Gf_0(x) + f_1(x) = g_1(x), \tag{3.27}$$

$$h\left\{f_0'(L) - f_0'(0)\right\} + f_2 = g_2. \tag{3.28}$$

From (3.27) we obtain the following formula for f_1:

$$f_1(x) = g_1(x) - Gg_0(x) \in L^2(0, L). \tag{3.29}$$

From (3.28) we obtain the expression for f_2 as

$$f_2 = g_2 - hg_0'(L). \tag{3.30}$$

Formulas (3.26), (3.29) and (3.30) yield the following formula for $\mathbb{A}^{-1}$:

$$\mathbb{A}^{-1} = \begin{bmatrix} 1 & 0 & 0 \\ -G & 1 & 0 \\ -h\{A\cdot|_L - A\cdot|_0\} & 0 & 1 \end{bmatrix} \tag{3.31}$$

Notice, the proof of the estimate $\|\mathbb{A}U\|_{\mathcal{H}} \le C_0\|U\|_{\mathcal{H}}$ did not depend on the signs of G and h. Thus, the estimate $\|\mathbb{A}^{-1}U\|_{\mathcal{H}} \le C_1\|U\|_{\mathcal{H}}$ follows immediately.

The lemma is shown. ■

Now we return to the evolution problem (3.10) and based on Lemma 3.2 rewrite it in the form of an evolution equation

$$\frac{d}{dt}U(x,t) = (\mathbb{L}U)(x,t), \tag{3.32}$$

with $\mathbb{L}$ being given by the following formula:

$$\mathbb{L} = \mathbb{A}^{-1}\mathbb{B} = \begin{bmatrix} 1 & 0 & 0 \\ -G & 1 & 0 \\ -h\{A\cdot|_L - A\cdot|_0\} & 0 & 1 \end{bmatrix} \begin{bmatrix} 0 & 1 & 0 \\ -E\frac{d^4}{dx^4} & 0 & 0 \\ 0 & 0 & -H \end{bmatrix}$$

$$= \begin{bmatrix} 0 & 1 & 0 \\ -E\frac{d^4}{dx^4} & -G & 0 \\ 0 & -h\left\{A.|_L - A.|_0\right\} & -H \end{bmatrix}. \tag{3.33}$$

In order to deal with symmetric or self-adjoint operators (rather than skew-symmetric or skew-self-adjoint operators), we will consider asymptotic and spectral properties of the operator

$$\mathcal{L} = -i\mathbb{L}. \tag{3.34}$$

With (3.34), the evolution equation now has the form:

$$\frac{d}{dt}U(x,t) = i\left(\mathcal{L}U\right)(x,t). \tag{3.35}$$

From now on, the main object of interest is the dynamics generator $\mathcal{L}$

$$\mathcal{L} = -i \begin{bmatrix} 0 & 1 & 0 \\ -E\frac{d^4}{dx^4} & -G & 0 \\ 0 & -h\left\{A\cdot|_L - A\cdot|_0\right\} & -H \end{bmatrix}. \tag{3.36}$$

$$\begin{aligned} \mathcal{D}(\mathcal{L}) = \Big\{ U = (u_0, u_1, u_2)^T \in \mathcal{H} : u_0 \in H^4(0,L) \cap H_0^2(0,L), u_1 \in H_0^2(0,L); \\ u_0'''(L) = 0, Eu_0''(L) = \Theta u_2 \Big\}. \end{aligned} \tag{3.37}$$

3.2 Spectral properties of $\mathcal{L}$

To describe the spectrum of the operator $\mathcal{L}$, we will find the formula for $\mathcal{L}^{-1}$. To this end, consider the following equation in $\mathcal{H}$

$$\mathcal{L}F = \mathbb{G}, \tag{3.38}$$

where

$$\mathbb{G}(x) = (g_0(x),\ g_1(x),\ g_2)^T \in \mathcal{H}.$$

Rewriting this equation component-wise, we obtain

$$f_1(x) = i\, g_0(x), \tag{3.39}$$

$$-Ef_0''''(x) - Gf_1(x) = i\, g_1(x), \tag{3.40}$$

$$-h\,(f_1'(L) - f_1'(0)) - Hf_2 = i\, g_2. \tag{3.41}$$

Since F must be from $\mathcal{D}(\mathcal{L})$, we have $f_1'(0) = 0$ and system can be reduced to

$$Ef_0''''(x) = -i\, g_1(x) - i\, Gg_0(x) \equiv g_3(x),\ g_3(x) \in L^2(0, L) \tag{3.42}$$

$$Hf_2 = -i\, g_2 - hf_1'(L) = -i\,(g_2 + hg_0'(L)). \tag{3.43}$$

Integrating equation (3.42) once and counting condition $f_0'''(L) = 0$, we get

$$Ef_0'''(x) = \int_0^L g_3(\xi)d\xi. \tag{3.44}$$

Integrate (3.44) again and have integrating equation (3.42) four times, we obtain

$$Ef_0(x) = \int_0^x d\xi \int_0^\xi d\eta \int_\eta^L d\tau \int_\tau^L g_3(\omega)d\omega + Ax^3 + Bx^2 + Cx + D, \tag{3.45}$$

where A, B, C, D are arbitrary constants.

For the component f_0 to satisfy two conditions at $x = 0,\ f_0(0) = f_0'(0) = 0$, we choose $C = D = 0$.

To satisfy the condition $f'''(L) = 0$, we choose $A = 0$. To specify B, we take into account the forth condition from (3.37), i.e., $Ef_0''(L) = \Theta f_2$.

Combining (3.39) and (3.41), we obtain

$$f_2 = -\frac{1}{H}(i\,g_2 + hf_1'(L)) = -\frac{1}{H}(i\,g_2 + i\,hg_0'(L)). \tag{3.46}$$

From (3.45), we get

$$Ef_0''(L) = 2B = -\Theta\frac{1}{H}\,(i\,g_2 + i\,hg_0'(L))$$

or

$$B = -\frac{i\,\Theta}{2H}\,(g_2 + hg_0'(L))\,.$$

Thus,

$$f_0(x) = \int_0^x d\xi \int_0^\xi d\eta \int_\eta^L d\tau \int_\tau^L g_3(\omega)d\omega - \frac{i\,\Theta}{2H}\,(g_2 + hg_0'(L))\,x^2, \tag{3.47}$$

$$f_1(x) = -i\,g_0(x), \tag{3.48}$$

$$f_2 = -\frac{i}{H}\,(g_2 + hg_0'(L))\,. \tag{3.49}$$

Finally, we check that (3.47)− (3.49) yield the desired solution. Indeed, function (3.47) satisfies equation (3.45).

To show that $F = (f_0, f_1, f_2)^T$ is from $\mathcal{D}(\mathcal{L})$, it remains to check the boundary conditions.

From (3.47) it follows that $f_0 \in H^4(0, L) \cap H_0^2(0, L)$,;

from (3.48) it follows that $f_1 \in H_0^2(0, L)$,

from (3.47) it follows that $f_0'''(L) = 0$.

Due to choice of B, the fourth boundary condition is satisfied.

Combining (3.47)− (3.49), we obtain the following formulas for the inverse operator $\mathcal{L}^{-1}$:

$$f_0(x) = \mathcal{R}\,(Gg_0 + g_1) - \frac{i\,\Theta}{2H}(g_2 + hg_0'(L))x^2,$$

$$f_1(x) = i\,g_0(x)$$

$$f_2 = -\frac{i}{H}(g_2 + hg_0'(L)).$$

Here $\mathcal{R}$ is a Volterra integral operator, i.e.,

$$\mathcal{R}(\psi) = \int_0^x d\xi \int_0^\xi d\eta \int_\eta^L d\tau \int_\tau^L \psi(\omega) d\omega.$$

To show that $\mathcal{L}^{-1}$ is compact, we note that the domain of $\mathcal{L}^{-1}$ is a closed subspace of the space $\mathcal{H}_1 = H^2(0,L) \times L^2(0,L) \times \mathbb{C}$ and the range is a closed subspace of the space $\mathcal{H}_2 = H^4(0,L) \times H^2(0,L) \times \mathbb{C}$.

It follows from the above proof that $\mathcal{L}^{-1}$ is a bounded operator from $\mathcal{H}$ into $\mathcal{D}(\mathcal{L})$ if $\mathcal{D}(\mathcal{L})$ is equipped with the norm of $\mathcal{H}_2$. Due to fact that embedding $\mathcal{H}_2 \subset \mathcal{H}_1$ is compact, one can conclude that the operator is compact. ■

From compactness of the embedding, we obtain that $\mathcal{L}^{-1}$ is compact operator. Thus, $\mathcal{L}$ has purely discrete spectrum of *normal eigenvalues*. Recall that an eigenvalue is normal if it is an isolated point of the spectrum with a finite multiplicity.

3.3 Non-dissipativity of $\mathcal{L}$

Definition 3.2. A linear operator T in a Hilbert space H is said to be *dissipative* if for any $F \in \mathcal{D}(T)$ the following inequality holds:

$$\Im(TF, F)_H \geq 0. \tag{3.50}$$

If for T, the estimate (3.50) is valid, then for operator $V = iT$, the following inequality is valid:

$$\Re(VF, F)_H \leq 0. \tag{3.51}$$

Any linear operator, for which (3.51) holds is said to be *accretive*.

Let $\mathbb{L} = i\mathcal{L}$ and we have

$$2\left(\mathbb{L}U,U\right)_{\mathcal{H}}=\left(\begin{pmatrix}u_1(x)\\ -Eu_0''''(x)-Gu_1(x)\\ -h\left(u_1'(L)-u_1'(0)\right)-Hu_2\end{pmatrix},\begin{pmatrix}u_0(x)\\ u_1(x)\\ u_2\end{pmatrix}\right)_{\mathcal{H}}$$

$$=\int_0^L Eu_1''(x)\overline{u_0''(x)}dx-\int_0^L\left[Eu_0''''(x)\overline{u_1(x)}+G|u_1(x)|^2\right]dx-\left[hu_1'(L)+Hu_2\right]\overline{u}_2 \tag{3.52}$$

To simplify (3.52), we use

$$\int_0^L u_0''''(x)\overline{u_1(x)}dx=\left(u_0'''\overline{u_1}\right)\Big|_0^L-u_0''\overline{u_1'}\Big|_0^L+\int_0^L u_0''(x)\overline{u_1''(x)}dx.$$

Since $U\in\mathcal{D}(\mathcal{L})$, we have $u_1(0)=u_1'(0)=0$ and $u_0'''(L)=0$, which yields

$$\int_0^L u_0''''(x)\overline{u_1(x)}dx=-u_0''(L)\overline{u_1'(L)}+\int_0^L u_0''(x)\overline{u_1''(x)}dx. \tag{3.53}$$

Substituting (3.53) into (3.52) we obtain

$$\begin{aligned}2(\mathbb{L}U,U)_{\mathcal{H}}=\int_0^L Eu_1''(x)\overline{u_0''(x)}-\int_0^L E\overline{u_1''(x)}u_0''(x)dx+Eu_0''(L)\overline{u_1'(L)}\\ -G\int_0^L|u_1(x)|^2dx-hu_1'(L)\overline{u_2}-H|u_2|^2.\end{aligned} \tag{3.54}$$

Using $Eu_0''(L)=\Theta u_2$, we have from (3.54)

$$2\Re(\mathbb{L}U,U)_{\mathcal{H}}=-G\|u_1\|_{L^2(0,L)}^2-H|u_2|^2+\Re\left\{\Theta u_2\overline{u_1'(L)}-hu_1'(L)\overline{u_2}\right\}. \tag{3.55}$$

It's clear that if $\Theta=h$, then $\Re(\mathbb{L}U,U)_{\mathcal{H}}\leq 0$.

3.4 Adjoint operator of dynamics generator

Definition 3.3. An operator $\mathcal{L}^*$ is called *an adjoint* to $\mathcal{L}$ if for any $U \in \mathcal{D}(\mathcal{L})$, there exists $V \in \mathcal{H}$ such that

$$(\mathcal{L}U, V)_{\mathcal{H}} = (U, \mathcal{L}^* V)_{\mathcal{H}}. \tag{3.56}$$

As is known, for any densely defined operator $\mathcal{L}$ there exists the unique adjoint $\mathcal{L}^*$.

The following result holds.

Lemma 3.4. *For the operator $\mathcal{L}$ defined by formulas (3.36) and (3.37) the adjoint operator $\mathcal{L}^*$ is defined by the differential expression*

$$\mathcal{L}^* = -i \begin{pmatrix} 0 & 1 & 0 \\ -E\frac{d^4}{dx^4} & G & 0 \\ 0 & -\Theta A \cdot |_L & H \end{pmatrix} \tag{3.57}$$

on the domain

$$\mathcal{D}(\mathcal{L}^*) = \Big\{ V = (v_0, v_1, v_2)^T \in \mathcal{H} : v_0 \in H^4(0,L) \cap H_0^2(0,L), v_1 \in H_0^2(0,L); \\ v_0'''(L) = 0, E v_0''(L) = h v_2. \Big\} \tag{3.58}$$

Proof. From (3.57), we obtain that

$$2i\,(\mathcal{L}U, V)_{\mathcal{H}} = 2 \left(\begin{pmatrix} u_1 \\ -Eu_0'''' - Gu_1 \\ -hu_1'(L) - Hu_2 \end{pmatrix}, \begin{pmatrix} v_0 \\ v_1 \\ v_2 \end{pmatrix} \right)_{\mathcal{H}} =$$

$$\int_0^L \left[Eu_1''(x)\overline{v_0''(x)} - Eu_0''''(x)\overline{v_1(x)} - Gu_1\overline{v_1} \right] dx - hu_1'(L)\overline{v_2} - Hu_2\overline{v_2}.$$

Integrating by parts the second integral, we get

$$2i(\mathcal{L}U,V)_{\mathcal{H}} = -Eu_0'''\overline{v_1}\Big|_0^L + Eu_0''\overline{v_1'}\Big|_0^L - hu_1'(L)\overline{v_2} - Hu_2\overline{v2} + I,$$

where

$$I = \int_0^L \left[Eu_1''(x)\overline{v_0''(x)} - Eu_0''(x)\overline{v_1''(x)} - Gu_1(x)\overline{v_1(x)}\right] dx. \tag{3.59}$$

Since $v_1(0) = v_1'(0) = u_0'''(L) = 0$ and $Eu_0''(L) = \Theta u_2$, we obtain the following expression for the out of integral terms: $\Theta u_2\overline{v_1'(L)} - hu_1'(L)\overline{v_2}$, which yields

$$2i(\mathcal{L}U,V)_{\mathcal{H}} = I + \Theta u_2\overline{v_1'(L)} - hu_1'(L)\overline{v_2} - Hu_2\overline{v_2}. \tag{3.60}$$

Now let us consider

$$-2i(U,\mathcal{L}^*V)_{\mathcal{H}} = 2\left(\begin{pmatrix} u_0 \\ u_1 \\ u_2 \end{pmatrix}, \begin{pmatrix} v_1 \\ -Ev_0'''' + Gv_1 \\ -\Theta v_1'(L) + Hv_2 \end{pmatrix}\right)_{\mathcal{H}}$$

$$= \int_0^L [Eu_0''(x)\overline{v_1''(x)} - Eu_1\overline{v_0''''(x)} + Gu_1(x)v_1(x)]dx - \Theta u_2\overline{v_1'(L)} + Hu_2\overline{v_2}.$$

Integrating by parts we obtain

$$-2i(U,\mathcal{L}^*V)_{\mathcal{H}} = -Eu_1\overline{v_0'''}\Big|_0^L + Eu_1'\overline{v_0''}\Big|_0^L - \Theta u_2\overline{v_1'(L)} + Hu_2\overline{v_2} + I_1,$$

where

$$I_1 = \int_0^L \left[Eu_0''(x)\overline{v_1''(x)} - Eu_1''(x)\overline{v_0''(x)} + Gu_1(x)\overline{v_1(x)}\right] dx. \tag{3.61}$$

Counting $u_1(0) = u_1'(0) = v'''(L) = 0$, we obtain that out of integral terms are

$$Eu_1'(L)\overline{v_0''(L)} - \Theta u_2\overline{v_1'(L)} + Hu_2\overline{v_2}. \tag{3.62}$$

Since $Ev_0''(L) = hv_2$, we reduce (3.62) to

$$hu_1'(L)\overline{v_2} - \Theta u_2\overline{v_1'(L)} + Hu_2\overline{v_2}. \tag{3.63}$$

With (3.63), we obtain

$$-2i(U, \mathcal{L}^*V)_{\mathcal{H}} = -hu_1'(L)\overline{v_2} - \Theta u_2 v_1'(L) + Hu_2\overline{v_2} + \mathcal{I}_1,$$

or

$$2i(U, \mathcal{L}^*V)_{\mathcal{H}} = hu_1'(L)\overline{v_2} + \Theta u_2 v_1'(L) - Hu_2\overline{v_2} - \mathcal{I}_1. \tag{3.64}$$

Since $I_1 = -I$ (see (3.59) and (3.61)), we obtain that $(\mathcal{L}U, V)_{\mathcal{H}} = (U, \mathcal{L}^*, V)_{\mathcal{H}}$.

The proof is complete. ■

CHAPTER 4

NUMERICAL SPECTRAL ANALYSIS OF DYNAMICS GENERATOR

In this section we present numerical scheme that allows us to obtain approximation for the eigenvalues of the operator $\mathcal{L}$. We use standard approximation of the matrix differential operator by a linear system in a finite dimensional space. Our main technical tool is approximation using Chebyshev polynomials. We start with brief outline of polynomial interpolation.

4.1 Polynomial interpolation

One of the straight-forward ways of obtaining a polynomial approximation of degree n to a given continuous function $f(x)$ on $[-1, 1]$ is to interpolate between the values of $f(x)$ at $n + 1$ suitably selected distinct points in the interval. For example, to interpolate at

$$x_1, x_2, \cdots, x_{n+1}$$

by the polynomial

$$p_n(x) = c_0 + c_1 x + \cdots + c_n x^n,$$

we require that

$$c_0 + c_1 x_k + \cdots + c_n x_k^n = f(x_k) \quad (k = 1, \cdots, n + 1) \tag{4.1}$$

The equations (4.1) are a set of $n + 1$ linear equations for the $n + 1$ coefficients $c_0, c_1, \cdots, c_n$ that define $p_n(x)$. Whatever the values of $f(x_k)$, the interpolating polynomial $p_n(x)$ exists

and is unique, since the determinant of the linear system (4.1) is non-zero. Specifically

$$det \begin{pmatrix} 1 & x_1 & x_1^2 & \cdots & x_1^n \\ 1 & x_2 & x_2^2 & \cdots & x_2^n \\ \vdots & \vdots & \vdots & \ddots & \vdots \\ 1 & x_{n+1} & x_{n+1}^2 & \cdots & x_{n+1}^n \end{pmatrix} = \prod_{j=1}^{n+1} (x_i - x_j) \neq 0.$$

It is generally not only rather time-consuming, but also numerically unstable, to determine $p_n(x)$ by solving (4.1) as it stands, and indeed many more efficient and reliable formulae for interpolation have been devised [15].

Some interpolation formulae are tailored to equally spaced points $x_1, x_2, \cdots, x_{n+1}$. Surprisingly however, if we have a free choice of interpolation points, it is not necessarily a good idea to choose them equally spaced. An obvious equally-spaced set for the interval $[-1, 1]$ is given for each value of n by

$$x_k = -1 + \frac{2k+1}{n+1} \quad (k = 0, \cdots, n). \tag{4.2}$$

These points are spaced a distance $\frac{2}{n+1}$ apart, with half spacings of $\frac{1}{n+1}$ between the first and the last points and the end points of the interval.

However, as was mentioned above the points (4.2) are not appropriate for all continuous functions $f(x)$ when n becomes large. The following example demonstrates the divergence of interpolation away from $f(x)$ as n increases (this typically occurs in an oscillating pattern that magnifies near the ends of the interpolation points). This phenomenon is attributed to Runge Carl David Tolm.

4.2 Runge's Phenomenon

The Weierstrass Approximation Theorem states that every continuous function f defined on an interval $[a, b]$ can be uniformly approximated as closely as desired by a polynomial

function $p_n(x)$ of sufficiently large degree of n, i.e.,

$$\lim_{n\to\infty}\left(\max_{a\le x\le b}|f(x)-p_n(x)|\right)=0.$$

When interpolation of a function with equidistant points is chosen, Runge's phenomenon demonstrates that interpolation can easily result in divergent approximation.

Theorem 4.1 (Runge phenomenon)

If x_k are chosen to be the points (4.2) *for each $n \geq 0$, then the interpolating polynomial $p_n(x)$ does not converge uniformly on $[-1,1]$ as $n \to \infty$ for the function $f(x) = 1/(1+ax^2)$, where $a > 1$.*

It can be proven that the interpolation error increases (without bound) when the degree of the polynomial is increased:

$$\lim_{n\to\infty}\left(\max_{-1\le x\le 1}|f(x)-p_n(x)|\right)=+\infty.$$

This result shows that high-degree polynomial interpolation at equidistant points can be troublesome. The graph below represents interpolation of the function $f(x) = 1/(1+25x^2)$ using equally spaced points on the interval $[-1,1]$.

The oscillation can be minimized by using nodes that are distributed more densely towards the edges of the interval, specifically, with asymptotic density (on the interval $[-1,1]$) given by the formula $1/\sqrt{1-x^2}$. A standard example of such a set of nodes is Chebyshev nodes, for which the maximum error approximating the Runge function is guaranteed to diminish with increasing polynomial order [16].

The set of zeros of the Chebyshev polynomial $T_{n+1}(x)$ (for the definition of Chebyshev polynomial, see Section 4.3 below):

$$x = x_k = \cos\left(\frac{(k-\frac{1}{2})\pi}{n+1}\right) \quad (k = 1, \cdots, n+1). \tag{4.3}$$

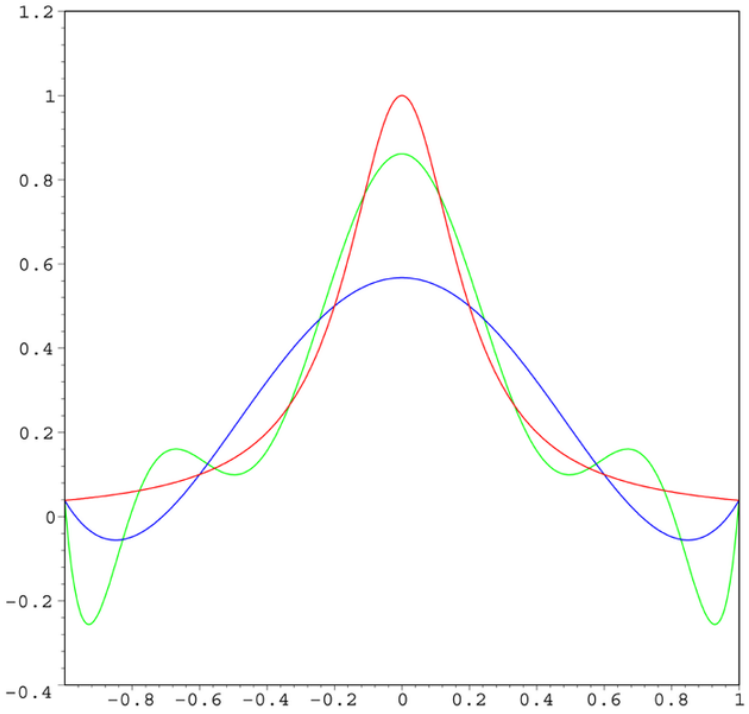

Figure 4.1: Interpolation to Runge function: the red curve is the Runge function. The blue curve is a 5th-order interpolating polynomial. The green curve is a 9th-order interpolating polynomial

By expressing the polynomial in terms of Chebyshev polynomials, this choice of interpolation points (4.3) can be made far more efficient and stable from a computational point a view than the equally-spaced set (4.2).

4.3 Chebyshev Polynomials

Definition 4.1. *The Chebyshev polynomial $T_n(x)$ of the first kind is a polynomial in x of degree n, defined by the relation*

$$T_n(x) = \cos n\theta, \tag{4.4}$$

when $x = \cos\theta$.

If the range of the variable x is the interval $[-1, 1]$, then the range of the corresponding variable θ can be taken as $[0, \pi]$. These ranges are traversed in opposite directions, since $x = -1$ corresponds to $\theta = \pi$ and $x = 1$ corresponds to $\theta = 0$.

It is well known (as a consequence of de Moivre's Theorem) that $cos\, n\theta$ is a polynomial of degree n in $cos\, \theta$, and indeed we are familiar with the elementary formulae

$$\cos 2\theta = 2\cos^2\theta - 1, \;\; \cos 3\theta = 4\cos^3\theta - 3\cos\theta, ...$$

We may immediately deduce from (4.4), that the first few Chebyshev polynomials are

$$T_0(x) = 1, \quad T_1(x) = x, \quad T_2(x) = 2x^2 - 1, \quad T_3(x) = 4x^3 - 3x, ... \tag{4.5}$$

Combining the trigonometric identity

$$\cos n\theta + \cos(n-2)\theta = 2\cos\theta cos(n-1)\theta$$

with Definition 4.1, we obtain the following recurrence relation:

$$T_n(x) = 2xT_{n-1}(x) - T_{n-2}(x), \quad n = 2, 3, \cdots, \tag{4.6}$$

which together with the initial conditions

$$T_0(x) = 1, \quad T_1(x) = x$$

recursively generates all the polynomials $\{T_n(x)\}$.

Thus, we have:

$$T_0 = 1$$

$$T_1 = x$$

$$T_2 = 2x^2 - 1$$

$$T_3 = 4x^3 - 3x$$

$$T_4 = 8x^4 - 8x^2 + 1$$

$$T_5 = 16x^5 - 16x^3 - x$$

$$\dots$$

4.4 Collocation method. Chebyshev Cardinal Functions

A general idea of a collocation method is such that a quantity is somehow 'sampled' at a set of grid-points. This approach is reminiscent of the finite difference method.

Suppose we have a set of data at a nonuniform, even randomly chosen set of gridpoints; a total of N points. A really useful thing in numerical analysis is a polynomial function that is zero at all but one of these points. The value of the polynomial function at the final remaining point could be anything but zero, but usually it is normalized to unity. If there was one of these functions for each of the gridpoints, then the collection of functions can be used for interpolation between the points.

Gridpoints are often chosen with the aid of special polynomials. Consider an ordinary expansion in Chebyshev plounomials,

$$u = \sum_{n=0}^{N} u_n T_n. \tag{4.7}$$

Next, one has to choose the set of grid-points.

Any oscillatory function suggests two possible grids: 1) the gridpoints where the function crosses zero, and 2) the gridpoints where the function is maxima.

Lets consider the grid defined by the maxima of a Chebyshev polynomial. The Chebyshev function, T_n, has $N-1$ positions where the derivative is zero. If the endpoints are also included, the the grid contains $N+1$ points, as required. The position of the interior points is determined by setting the derivative T_N to zero, and solving for x, which results in

$$x_j = \cos\frac{j\pi}{N}, \quad (j = 0, 1, \cdots, N). \tag{4.8}$$

These are the well-known Chebyshev-Gauss-Lobatto points. Cardinal functions may be defined by

$$\psi(x) = (-1)^{k+1}\frac{(1-x^2)T_N'(x)}{c_k N^2(x-x_k)}, \tag{4.9}$$

where:

$$c_k = \begin{cases} 2, & if \;\; k = 0, \\ 1, & otherwise. \end{cases}$$

We use such cardinal functions approximate eigenvalues of the differential operator. To this end, we introduce discrete version of a derivative.

4.5 Differentiation matrices

Suppose that we know the values of any nth degree polynomial $p(x)$ at $n+1$ points $x_0, \cdots, x_n$. Then these values determine the polynomial uniquely, and so determine the values of the derivatives $p'(x) = dp(x)/dx$ at the same $n+1$ points. Each such derivative can, in fact, be expressed as a fixed linear combination of the given function values, and the whole relationship written in matrix form:

$$\begin{pmatrix} p'(x_0) \\ \vdots \\ p'(x_n) \end{pmatrix} = \begin{pmatrix} d_{0,0} & \cdots & d_{0,n} \\ \vdots & \ddots & \vdots \\ d_{n,0} & \cdots & d_{n,n} \end{pmatrix} \begin{pmatrix} p(x_0) \\ \vdots \\ p(x_n) \end{pmatrix}, \tag{4.10}$$

where $\mathbf{D}=\{d_{j,k}\}_{j,k=0}^{n}$ is called a *differentiation matrix*.

To find the differentiation matrix for the functions given by (4.9) we have to evaluate the derivative of each function. The derivative is

$$\frac{d\psi_k(x)}{dx} = \frac{(-1)^{k+1}}{c_k N^2}\left[\frac{-2xT_N^{'}(x)}{x-x_k} + \frac{(1-x^2)T_N^{''}(x)}{x-x_k} - \frac{(1-x^2)T_N^{'}(x)}{(x-x_k)^2}\right]. \tag{4.11}$$

The second derivative is most easily evaluated from the governing equation for Chebyshev polynomials:

$$T_N^{''}(x) = \frac{x}{1-x^2}T_N^{'}(x) - \frac{N^2}{1-x^2}T_N(x),$$

resulting in

$$\frac{d\psi_k(x)}{dx} = \frac{(-1)^{k+1}}{c_j N^2}\left[\frac{x(x-x_k)+(1-x^2)}{(x-x_k)^2}T_N^{'}(x) + \frac{N^2}{1-x^2}T_N(x)\right], \tag{4.12}$$

a rather complex result. However, evaluating this at the gridpoints, x_j, results in

$$\frac{d\psi_k}{dx}\Big|_{x_j} = \frac{(-1)^{j+k}c_j}{c_k(x_j-x_k)}.$$

This expression works as long as $j \neq k$. For $j = k$, (4.12) must be reexamined, resulting in

$$d_{j,k} = \begin{cases} \frac{1+2N^2}{6}, & j=k=0, \\ -\frac{1+2N^2}{6}, & j=k=N, \\ -\frac{x_k}{2(1-x_k^2)}, & j=k, 0<k<N, \\ \frac{(-1)^{j+k}c_j}{c_k(x_j-x_k)}, & j\neq k. \end{cases} \tag{4.13}$$

The differentiation matrix can be filled component-wise with the elements $d_{j,k}$, $0 \leq j \leq N$,

$0 \leq k \leq N$. Applying matrix D to the equation:

$$\begin{pmatrix} p'(x_0) \\ \vdots \\ p'(x_n) \end{pmatrix} = \mathbf{D} \begin{pmatrix} p(x_0) \\ \vdots \\ p(x_n) \end{pmatrix},$$

and obtain a similar relationship for the second derivatives

$$\begin{pmatrix} p''(x_0) \\ \vdots \\ p''(x_n) \end{pmatrix} = \mathbf{D^2} \begin{pmatrix} p(x_0) \\ \vdots \\ p(x_n) \end{pmatrix},$$

and keep the process to approximate higher order derivatives.

4.6 Eigenvalue problem for dynamics generator

Matrix eigenvalue problems arise in a large number of disciplines of sciences and engineering. They constitute the basic tool used in designing buildings, bridges, and turbines, that are resistant to vibrations. They allow to model queueing networks, and to analyze stability of electrical networks or fluid flow. They also allow the scientist to understand local physical phenomena or to study bifurcation patterns in dynamical system.

Lets approximate the eigenvalues of dynamics generator $\mathcal{L}$ by considering its action on a finite dimensional subspace $\mathcal{H}_N \in \mathcal{H}$. Namely, $\mathcal{H}_N$ consists of vectors of polynomials of degree $N-1$ and each polynomial determined uniquely by its values at the N points:

$$0 < x_1 < \cdots < x_j < \cdots < x_N = L$$

We use Chebyshev-Gauss-Lobatto grid (4.8):

$$x_j^{'} = \cos \frac{j\pi}{N-1} \quad (j = 0, 1, \cdots, N-1),$$

and transform the interval $[-1, 1]$ to $[0, L]$ by the following equation:

$$x_{j+1} = \frac{L}{2}(x_j^{'} + 1) \quad (j = 0, 1, \cdots, N-1).$$

Let

$$\Psi = \begin{bmatrix} \psi_0 \\ \psi_1 \\ \psi_2 \end{bmatrix},$$

be a three-component vector where ψ_0 and ψ_1 are polynomials of degree $N-1$ on $0 \leq x \leq L$, and ψ_2 is a constant.

Eigenvalue problem for dynamics generator $\mathbb{L}$ on $\mathcal{H}_N$ is

$$(\mathbb{L} - \lambda I)\,\Psi(x_j) = (\mathbb{L} - \lambda I) \begin{bmatrix} \psi_0(x_j) \\ \psi_1(x_j) \\ \psi_2 \end{bmatrix} = 0, \quad 1 \leq j \leq N. \tag{4.14}$$

In matrix form, the eigenvalue problem is:

$$\mathbb{L} \begin{bmatrix} \psi_0 \\ \psi_1 \\ \psi_2 \end{bmatrix} = -i \begin{bmatrix} 0 & 1 & 0 \\ -ED^4 & -G & 0 \\ 0 & -h\{D_N^1 - D_1^1\} & -H \end{bmatrix} \begin{bmatrix} \psi_0 \\ \psi_1 \\ \psi_2 \end{bmatrix} = \lambda \begin{bmatrix} \psi_0 \\ \psi_1 \\ \psi_2 \end{bmatrix}, \tag{4.15}$$

where D^4- the fourth order differentiation matrix and D_j^n is the $j-$th row of differentiation matrix D of order n defined by Eq.(4.13).

Then $\mathbb{L}$ has size $(2N+1) \times (2N+1)$.

Indeed, the dynamics generator $\mathbb{L}$ on $\mathcal{H}_N$ has a form:

$$L = -i * \begin{pmatrix} \begin{bmatrix} 0 & 0 & \cdots & 0 \\ 0 & 0 & \cdots & 0 \\ \vdots & & \ddots & 0 \\ 0 & 0 & \cdots & 0 \end{bmatrix} & \begin{bmatrix} 1 & 0 & \cdots & 0 \\ 0 & 1 & \cdots & 0 \\ \vdots & & \ddots & 0 \\ 0 & 0 & \cdots & 1 \end{bmatrix} & \begin{bmatrix} 0 \\ 0 \\ \vdots \\ 0 \end{bmatrix} \\ -ED^4 & -G \begin{bmatrix} 1 & 0 & \cdots & 0 \\ 0 & 1 & \cdots & 0 \\ \vdots & & \ddots & 0 \\ 0 & 0 & \cdots & 1 \end{bmatrix} & \begin{bmatrix} 0 \\ 0 \\ \vdots \\ 0 \end{bmatrix} \\ \begin{bmatrix} 0 & 0 \cdots & 0 \end{bmatrix} & -h(D_N^1 - D_1^1) & -H \end{pmatrix}$$

4.7 Imposing the boundary conditions

Introduce a subspace X_N of $\mathcal{H}_N$ satisfying the boundary conditions:

$$X_N \subset \mathcal{H}_N \cap \mathcal{D}(\mathcal{L}),$$

where $\mathcal{D}(\mathcal{L})-$ domain of dynamics generator $\mathcal{L}$.

The eigenvalue problem for dynamics generator is restricted to subspace X_N.

We are interested in the eigenvalues for which the following is true: if $\mathcal{L}\Psi_k \in X_N$, then Ψ_k is an eigenvalue of $\mathcal{L}|_{X_N}$. Lets define row vectors of length N:

$$r_0 = [0, \quad 0, \quad 0, \cdots, 0, \quad 0],$$

$$r_1 = [1, \quad 0, \quad 0, \cdots, 0, \quad 0].$$

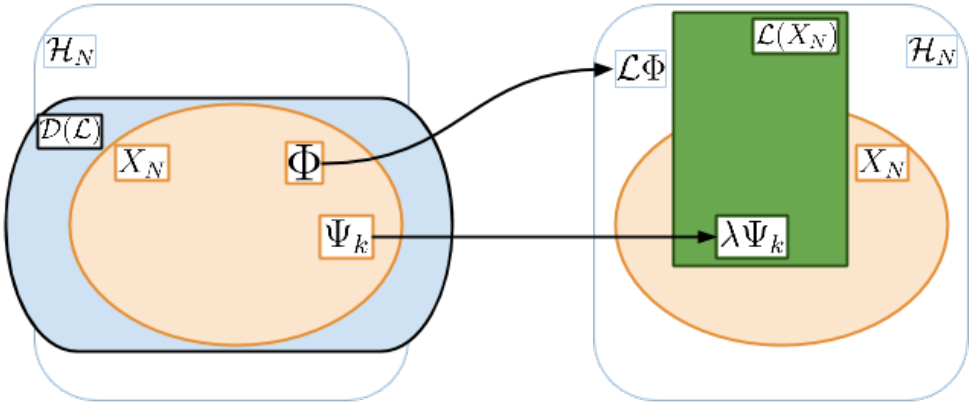

Figure 4.2: Eigenvalues of dynamics generator with boundary conditions

And let D_j^n be the $j-$th row of differentiation matrix D of order n defined by Eq.(4.13).

Then boundary conditions (3.6) and (3.7):

$$\left\{\begin{array}{c} \psi_0(0) = 0 \\ \psi_0'(0) = 0 \\ \psi_0'''(L) = 0 \\ E\psi_0''(L) - \Theta\psi_2 = 0 \end{array}\right\}$$

can be written as:

$$\Lambda\Psi = \begin{bmatrix} r_1 & r_0 & 0 \\ D_1^1 & r_0 & 0 \\ D_N^3 & r_0 & 0 \\ ED_N^2 & r_0 & -\Theta \end{bmatrix} \begin{bmatrix} \psi_0 \\ \psi_1 \\ \psi_2 \end{bmatrix} = 0. \tag{4.16}$$

The size of Λ is $4 \times (2N+1)$.

Then X_N is the kernel of the matrix.

Let B is a matrix, which columns is orthonormal basis for the kernel of Λ.

The subspace X_N is therefore generated by linear combinations of the k columns of B.

And the size of matrix B is $(2N+1) \times (2N-3)$.

Now the eigenvalue problem for dynamics generator with imposed boundary conditions has

form:

$$B^t \mathbb{L} B \, \Psi = \lambda \Psi. \tag{4.17}$$

The size of $B^t \mathbb{L} B$ is $(2N-3) \times (2N-3)$.

The described process implemented and results derived in numerical computing environment MATLAB (See Appendix A).

4.8 Numerical results of the model

We present the results of numerical approximation for the discretized continuous eigenvalue problem.

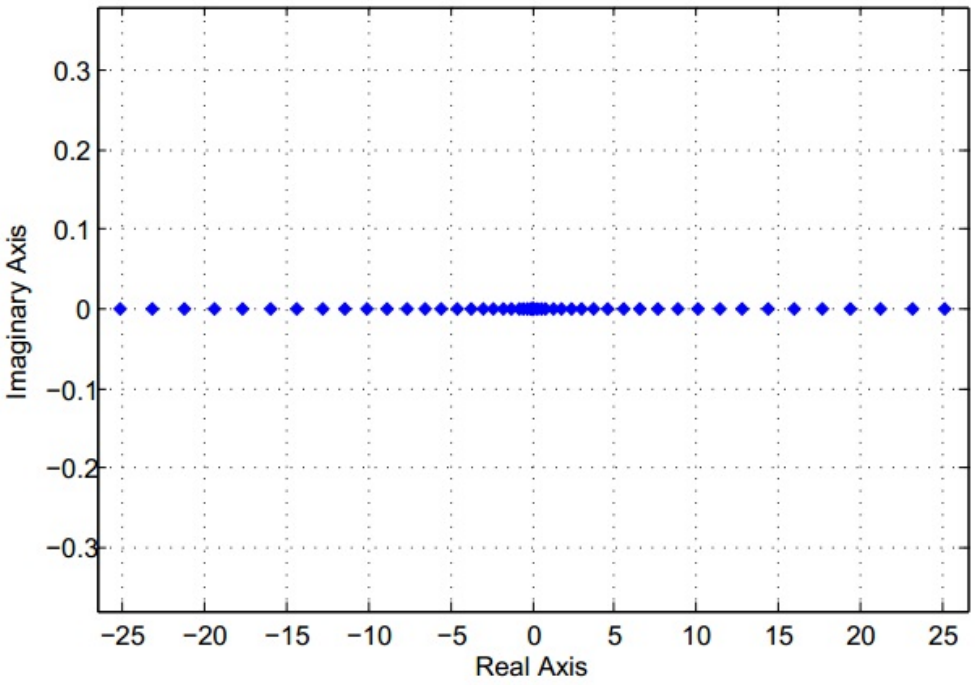

Figure 4.3: Undamped piezomechanic model

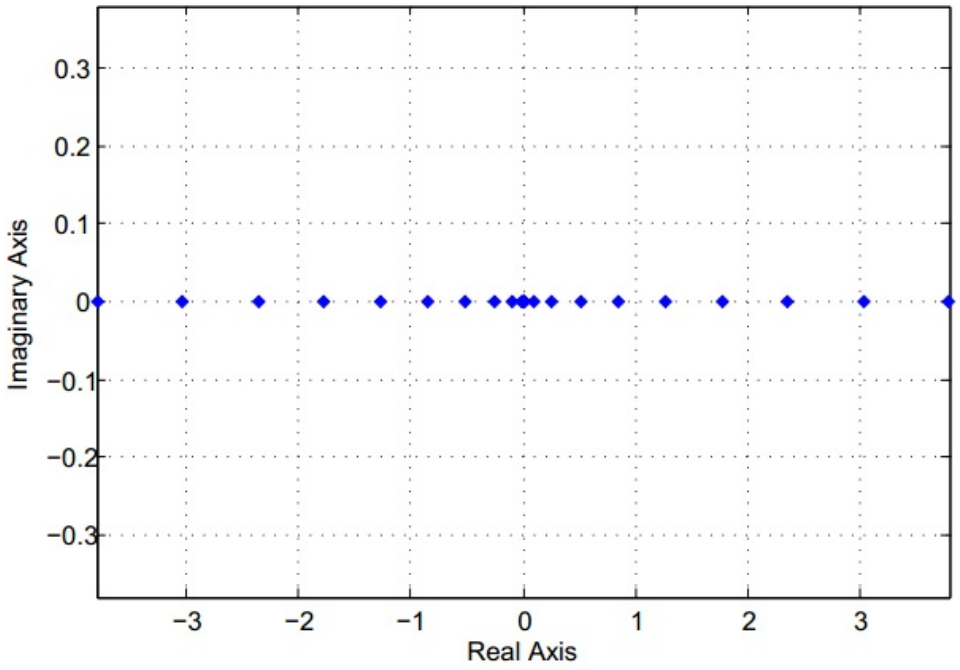

Figure 4.4: Undamped piezomechanic model. On a small scale

λ_n	$N = 60$	$N = 70$	$\frac{\lambda_{n+1}-\lambda_n}{n}$, $N = 60$	$\frac{\lambda_{n+1}-\lambda_n}{n}$, $N = 70$
λ_1	0.0000 + 0.0000i	0.0000 + 0.0000i	1.40e-14	8.41e-14
λ_2	1.1178e-14 - 8.4303e-15i	1.7542e-14 - 8.2252e-14i	1.58e-14	6.36e-14
λ_3	1.8656e-14 + 2.2255e-14i	8.7625e-15 + 4.4603e-14i	0.004	0.031
λ_4	0.0149 - 9.9499e-11i	0.0934 + 6.0939e-11i	0.019	0.019
λ_5	0.0934 - 3.7379e-12i	0.0149 + 6.7193e-10i	0.033	0.049
λ_6	0.2617 - 7.5567e-12i	0.2617 - 6.8829e-12i	0.041	0.041
λ_7	0.5129 + 1.3895e-12i	0.5129 - 9.5241e-12i	0.047	0.047
λ_8	0.8479 - 7.0308e-14i	0.8479 - 1.0553e-11i	0.052	0.052
λ_9	1.2666 + 4.3624e-13i	1.2666 + 9.1661e-13i	0.055	0.055
λ_{10}	1.7691- 2.8868e-13i	1.7691 - 2.0069e-12i	0.058	0.058
λ_{11}	2.3553 - 2.4107e-13i	2.3553 - 3.8258e-12i	0.060	0.060
λ_{12}	3.0253 + 2.5245e-13i	3.0253 - 1.0147e-12i	0.062	0.062
λ_{13}	3.7790 + 7.8947e-14i	3.7790 + 5.4636e-13i	0.064	0.064
λ_{14}	4.6165 + 2.3626e-14i	4.6165 - 1.8593e-13i	0.065	0.065
λ_{15}	5.5377 - 1.0165e-13i	5.5377 + 2.1306e-13i	0.066	0.066
λ_{16}	6.5426 - 7.4249e-15i	6.5426 - 1.6775e-13i	0.068	0.068
λ_{17}	7.6313 - 4.8209e-14i	7.6313 - 4.0984e-14i	0.068	0.068
λ_{18}	8.8038 + 7.7210e-14i	8.8038 - 1.4109e-13i	0.069	0.069
λ_{19}	10.0600 + 3.6142e-14i	10.0600 - 2.9172e-13i	0.070	0.070
λ_{20}	11.3999 - 4.2096e-14i	11.3999 - 1.0303e-13i	0.071	0.071
λ_{21}	12.8236 - 1.5656e-14i	12.8236 - 3.0329e-13i	0.071	0.071
λ_{22}	14.3310 + 7.0368e-14i	14.3310 + 4.0664e-14i	0.072	0.072
λ_{23}	15.9222 + 5.5805e-15i	15.9222 - 1.7172e-13i	0.072	0.072

Table 4.1: Undamped piezomechanic model

λ_n	$N = 60$	$N = 70$	$\frac{\lambda_{n+1}-\lambda_n}{n}$, $N = 60$	$\frac{\lambda_{n+1}-\lambda_n}{n}$, $N = 70$
λ_{24}	17.5972 - 1.1863e-15i	17.5972 - 2.4912e-13i	0.073	0.073
λ_{25}	19.3558 - 7.0834e-15i	19.3558 + 6.9481e-14i	0.073	0.073
λ_{26}	21.1983 - 2.8092e-15i	21.1983 + 3.1297e-14i	0.074	0.074
λ_{27}	23.1244 - 1.8955e-15i	23.1244 + 7.6238e-14i	0.074	0.074
λ_{28}	25.1343 + 1.5801e-14i	25.1343 + 3.8089e-14i	0.074	0.074
λ_{29}	27.2280 - 5.1967e-16i	27.2280 + 2.8158e-14i	0.075	0.075
λ_{30}	29.4054 - 2.2128e-15i	29.4054 + 5.7786e-14i	0.075	0.075
λ_{31}	31.6664 + 1.2234e-14i	31.6665 - 4.7646e-14i	0.075	0.075
λ_{32}	34.0111 + 1.6490e-14i	34.0114 + 4.0841e-14i	0.075	0.075
λ_{33}	36.4419 - 5.0280e-15i	36.4401 - 1.8352e-14i	0.076	0.076
λ_{34}	38.9563 + 4.1681e-15i	38.9525 + 9.0370e-15i	0.075	0.075
λ_{35}	41.5350 + 4.2343e-15i	41.5486 + 1.6474e-14i	0.076	0.076
λ_{36}	44.2024 + 7.8713e-15i	44.2285 - 2.9224e-14i	0.080	0.076
λ_{37}	47.0890 + 1.4041e-15i	46.9919 - 8.3033e-15i	0.079	0.076
λ_{38}	50.0178 + 4.7489e-15i	49.8390 - 1.3621e-14i	0.075	0.077
λ_{39}	52.8683 + 4.6258e-16i	52.7731 - 9.3165e-15i		0.077
λ_{40}		55.7905 + 2.2980e-14i		0.077
λ_{41}		58.8680 - 5.5113e-15i		0.076
λ_{42}		62.0366 + 8.4595e-15i		0.077
λ_{43}		65.4343 - 1.7009e-15i		0.080
λ_{44}		68.8661 + 9.6938e-16i		0.079
λ_{45}		72.1592 - 9.7123e-15i		0.074
λ_{46}		75.6472 - 1.3909e-16i		

Table 4.2: Undamped piezomechanic model (continuation)

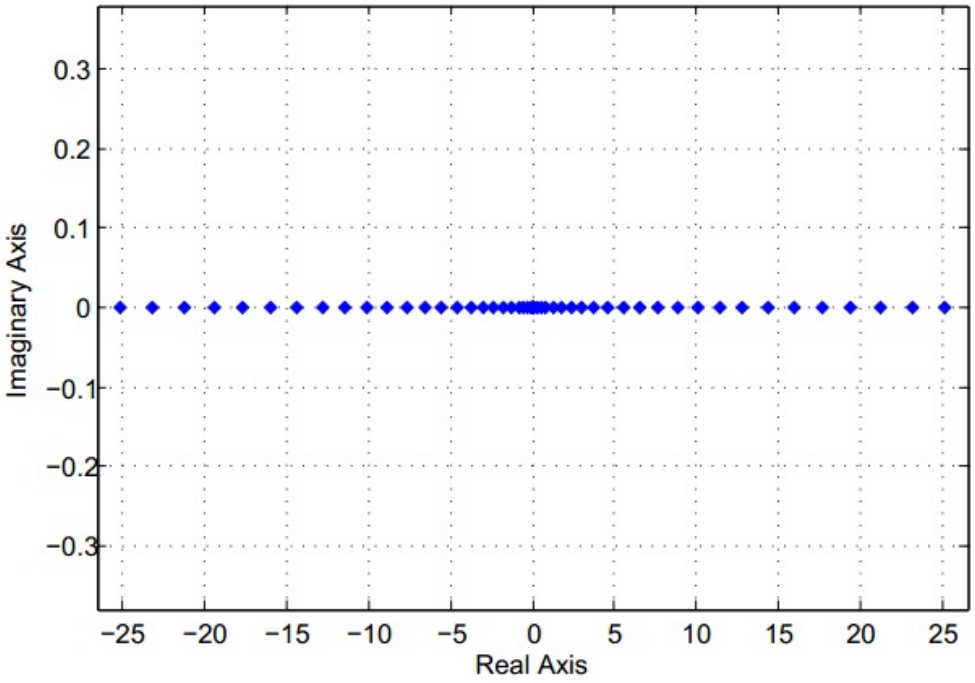

Figure 4.5: Damped piezomechanic model

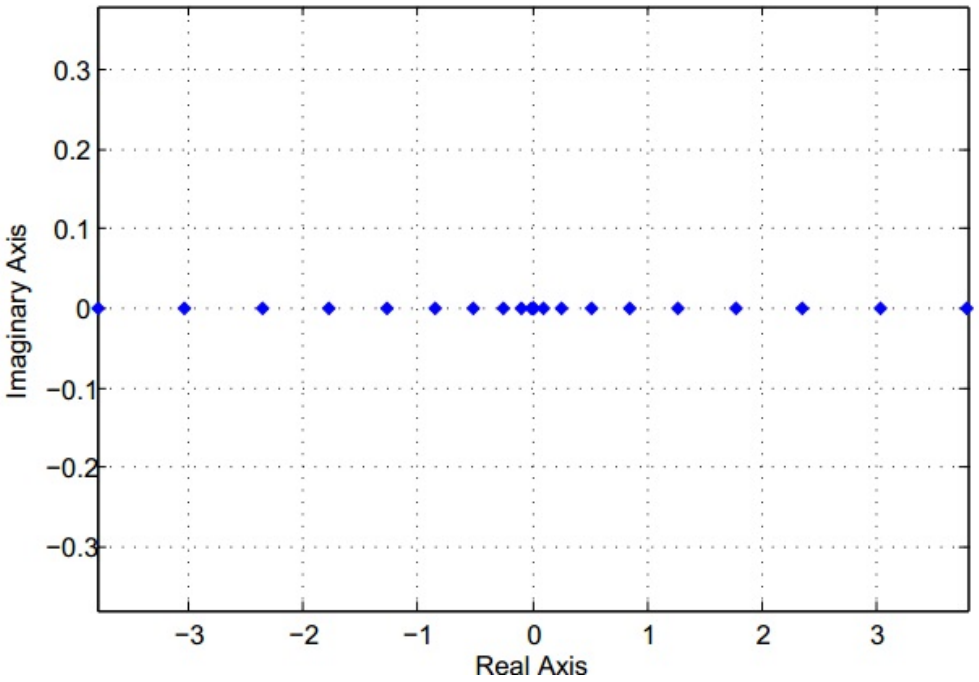

Figure 4.6: Damped piezomechanic model. On a small scale

λ_n	$N = 60$	$N = 70$	$\frac{\lambda_{n+1}-\lambda_n}{n}$, $N = 60$	$\frac{\lambda_{n+1}-\lambda_n}{n}$, $N = 70$
λ_1	0.0000 + 0.0000i	0.0000 + 0.0000i	0.000	0.000
λ_2	3.3157e-14 + 1.6964e-14i	9.9805e-14 + 7.0396e-15i	0.007	3.99e-14
λ_3	0.0149 + 3.6917e-11i	2.7676e-14 + 4.1341e-14i	0.026	0.004
λ_4	0.0934 - 1.4170-11i	0.0149 - 1.3065e-10i	0.042	0.019
λ_5	0.2617 - 1.9769e-12i	0.0934 - 2.1224e-12i	0.050	0.033
λ_6	0.5129 + 9.0488e-14i	0.2617 + 1.1438e-11i	0.055	0.041
λ_7	0.8479 + 2.7207e-12i	0.5129 - 3.7688e-13i	0.059	0.047
λ_8	1.2666 + 2.2069e-13i	0.8479 + 8.8944e-13i	0.062	0.052
λ_9	1.7691 + 1.9861e-13i	1.2666 - 2.0533e-12i	0.065	0.055
λ_{10}	2.3553 + 9.5399e-13i	1.7691 - 3.5539e-13i	0.066	0.058
λ_{11}	3.0253 + 2.9585e-14i	2.3553 + 9.8168e-13i	0.068	0.060
λ_{12}	3.7790 - 1.0146e-13i	3.0253 - 3.8272e-13i	0.069	0.062
λ_{13}	4.6165 + 7.9675e-16i	3.7790 - 8.5718e-13i	0.070	0.064
λ_{14}	5.5377 + 8.9854e-14i	4.6165 - 6.7076e-13i	0.071	0.065
λ_{15}	6.5426 + 1.4159e-14i	5.5377 - 5.2309e-13i	0.072	0.066
λ_{16}	7.6313 - 2.6575e-14i	6.5426 + 2.4187e-13i	0.073	0.068
λ_{17}	8.8038 - 9.7690e-15i	7.6313 + 1.2319e-13i	0.073	0.068
λ_{18}	10.0600 + 1.8712e-14i	8.8038 - 1.9349e-14i	0.074	0.069
λ_{19}	11.3999 + 1.5534e-14i	10.0600 + 5.6769e-14i	0.074	0.070
λ_{20}	12.8236 + 1.0866e-14i	11.3999 - 9.2537e-14i	0.075	0.071
λ_{21}	14.3310 + 1.8950e-15i	12.8236 + 1.0520e-13i	0.075	0.071
λ_{22}	15.9222 - 2.8381e-14i	14.3310 + 1.4238e-13i	0.076	0.072
λ_{23}	17.5972 - 2.0682e-14i	15.9222 + 6.8320e-14i	0.076	0.072

Table 4.3: Damped piezomechanic model

λ_n	$N = 60$	$N = 70$	$\frac{\lambda_{n+1}-\lambda_n}{n}$, $N = 60$	$\frac{\lambda_{n+1}-\lambda_n}{n}$, $N = 70$
λ_{24}	19.3558 - 1.9884e-15i	17.5972 - 2.0518e-14i	0.076	0.073
λ_{25}	21.1983 + 1.1772e-14i	19.3558 + 9.6973e-14i	0.077	0.073
λ_{26}	23.1244 - 2.3264e-14i	21.1983 + 5.5573e-14i	0.077	0.074
λ_{27}	25.1343 - 1.5279e-14i	23.1244 + 5.0955e-14i	0.077	0.074
λ_{28}	27.2280 - 1.9047e-14i	25.1343 + 1.6726e-14i	0.077	0.074
λ_{29}	29.4054 - 1.2267e-14i	27.2280 - 1.8820e-15i	0.077	0.075
λ_{30}	31.6664 - 4.8265e-15i	29.4054 + 2.6171e-14i	0.078	0.075
λ_{31}	34.0111 - 8.1893e-15i	31.6665 + 3.3840e-14i	0.078	0.075
λ_{32}	36.4419 - 2.3833e-15i	34.0114 + 4.3198e-14i	0.078	0.075
λ_{33}	38.9563 - 1.8641e-15i	36.4401 + 3.8385e-14i	0.078	0.076
λ_{34}	41.5350 - 1.1120e-15i	38.9525 + 1.8966e-14i	0.078	0.076
λ_{35}	44.2024 - 3.2730e-15i	41.5486 - 4.0433e-15i	0.082	0.076
λ_{36}	47.0890 - 3.6001e-15i	44.2285 - 3.2537e-15i	0.081	0.076
λ_{37}	50.0178 - 3.1468e-15i	46.9919 + 5.5665e-16i	0.077	0.076
λ_{38}	52.8683 - 1.7755e-15i	49.8390 - 1.1602e-15i	0.077	0.077
λ_{39}	55.8687 + 3.0378e-16i	52.7731 - 2.1036e-15i		0.077
λ_{40}		55.7905 + 3.3478e-15i		0.076
λ_{41}		58.8680 - 2.8635e-15i		0.077
λ_{42}		62.0366 - 7.4914e-15i		0.080
λ_{43}		65.4343 - 5.4235e-15i		0.079
λ_{44}		68.8661 - 6.4411e-15i		0.074
λ_{45}		72.1592 + 1.2540e-15i		0.077
λ_{46}		75.6472 - 1.1657e-15i		

Table 4.4: Damped piezomechanic model (continuation)

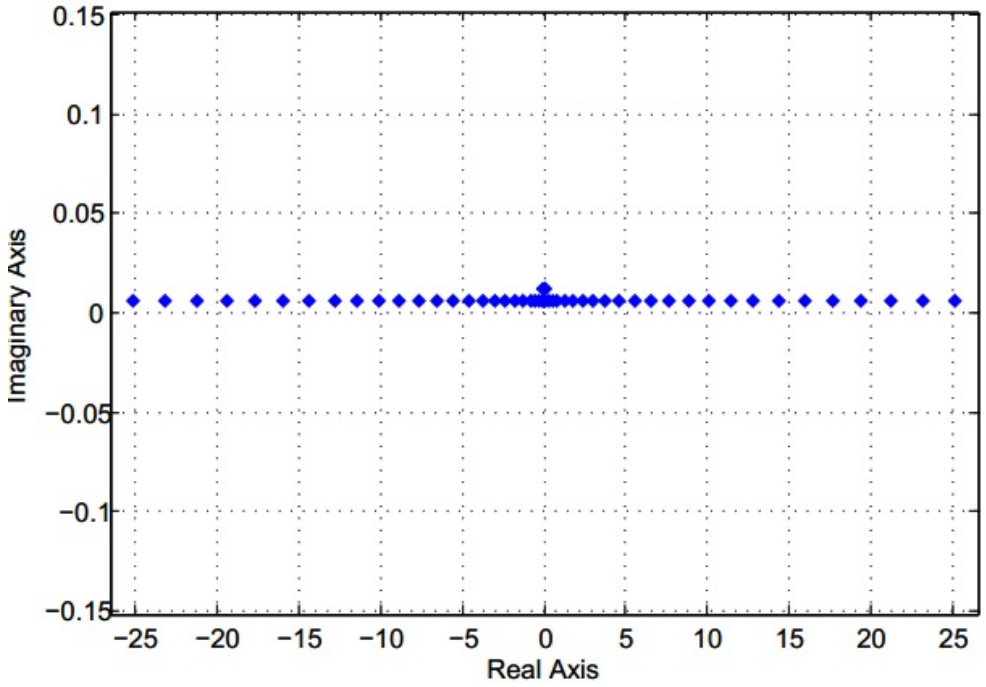

Figure 4.7: Undamped Euler-Benoulli beam model

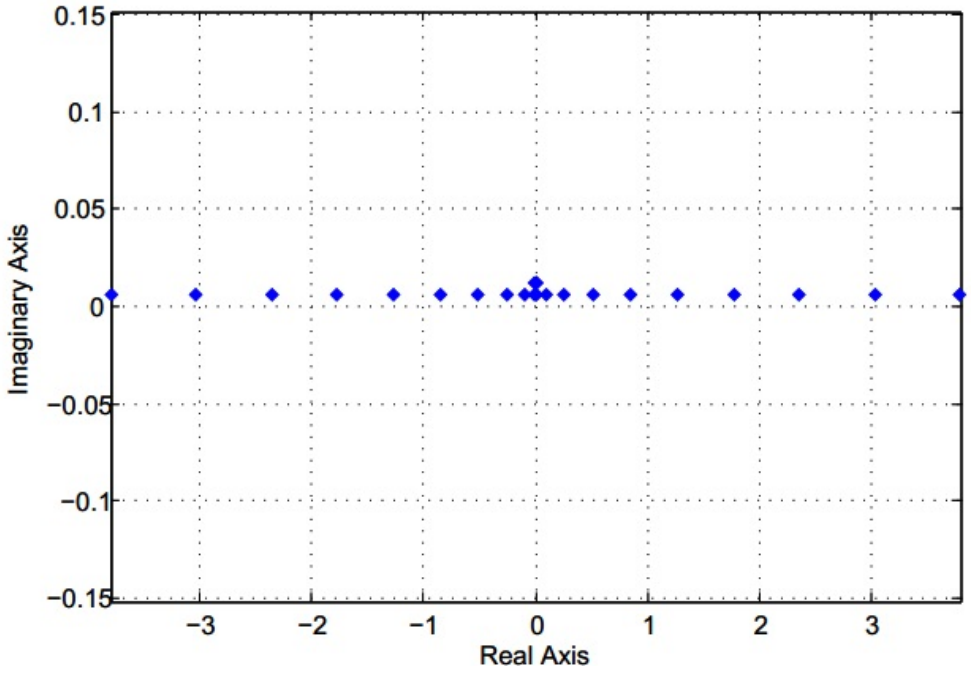

Figure 4.8: Undamped Euler-Benoulli beam model. On a small scale

λ_n	$N = 60$	$N = 70$	$\frac{\lambda_{n+1}-\lambda_n}{n}$, $N = 60$	$\frac{\lambda_{n+1}-\lambda_n}{n}$, $N = 70$
λ_1	0.0000 + 0.0000i	0.0000 + 0.0000i	0.012	0.012
λ_2	2.5791e-14 + 0.01249i	3.8444e-14 + 0.0125i	0.007	4.01e-14
λ_3	0.0135 + 0.0062i	2.9689e-14 + 0.0125i	0.026	0.004
λ_4	0.0932 + 0.0062i	0.0135 + 0.0062i	0.042	0.019
λ_5	0.2616 + 0.0062i	0.0932 + 0.0062i	0.050	0.033
λ_6	0.5129 + 0.0062i	0.2616 + 0.0062i	0.055	0.041
λ_7	0.8479 + 0.0062i	0.5129 + 0.0062i	0.059	0.047
λ_8	1.2666 + 0.0062i	0.8479 + 0.0062i	0.062	0.052
λ_9	1.7691 + 0.0062i	1.2666 + 0.0062i	0.065	0.055
λ_{10}	2.3553 + 0.0062i	1.7691 + 0.0062i	0.066	0.058
λ_{11}	3.0253 + 0.0062i	2.3553 + 0.0062i	0.068	0.060
λ_{12}	3.7790 + 0.0062i	3.0253 + 0.0062i	0.069	0.062
λ_{13}	4.6165 + 0.0062i	3.7790 + 0.0062i	0.070	0.064
λ_{14}	5.5377 + 0.0062i	4.6165 + 0.0062i	0.071	0.065
λ_{15}	6.5426 + 0.0062i	5.5377 + 0.0062i	0.072	0.066
λ_{16}	7.6313 + 0.0062i	6.5426 + 0.0062i	0.073	0.068
λ_{17}	8.8038 + 0.0062i	7.6313 + 0.0062i	0.073	0.068
λ_{18}	10.0600 + 0.0062i	8.8038 + 0.0062i	0.074	0.069
λ_{19}	11.3999 + 0.0062i	10.0600 + 0.006i	0.074	0.070
λ_{20}	12.8236 + 0.0062i	11.3999 + 0.0062i	0.075	0.071
λ_{21}	14.3310 + 0.0062i	12.8236 + 0.0062i	0.075	0.071
λ_{22}	15.9222 + 0.0062i	14.3310 + 0.0062i	0.076	0.072
λ_{23}	17.5972 + 0.0062i	15.9222 + 0.0062i	0.076	0.072

Table 4.5: Undamped Euler-Benoulli beam model

λ_n	$N = 60$	$N = 70$	$\frac{\lambda_{n+1}-\lambda_n}{n}$, $N = 60$	$\frac{\lambda_{n+1}-\lambda_n}{n}$, $N = 70$
λ_{24}	19.3558 + 0.0062i	17.5972 + 0.0062i	0.076	0.073
λ_{25}	21.1982 + 0.0062i	19.3558 + 0.0062i	0.077	0.073
λ_{26}	23.1244 + 0.0062i	21.1982 + 0.0062i	0.077	0.074
λ_{27}	25.1343 + 0.0062i	23.1244 + 0.0062i	0.077	0.074
λ_{28}	27.2280 + 0.0062i	25.1343 + 0.0062i	0.077	0.074
λ_{29}	29.4054 + 0.0062i	27.2280 + 0.0062i	0.077	0.075
λ_{30}	31.6664 + 0.0062i	29.4054 + 0.0062i	0.078	0.075
λ_{31}	34.0111 + 0.0062i	31.6665 + 0.0062i	0.078	0.075
λ_{32}	36.4419 + 0.0062i	34.0114 + 0.0062i	0.078	0.075
λ_{33}	38.9563 + 0.0062i	36.4401 + 0.0062i	0.078	0.076
λ_{34}	41.5350 + 0.0062i	38.9525 + 0.0062i	0.078	0.076
λ_{35}	44.2024 + 0.0062i	41.5486 + 0.0062i	0.082	0.076
λ_{36}	47.0890 + 0.0062i	44.2285 + 0.0062i	0.081	0.076
λ_{37}	50.0178 + 0.0062i	46.9919 + 0.0062i	0.077	0.076
λ_{38}	52.8683 + 0.0062i	49.8390 + 0.0062i	0.078	0.077
λ_{39}	55.8687 + 0.0062i	52.7731 + 0.0062i		0.077
λ_{40}		55.7905 + 0.0062i		0.076
λ_{41}		58.8680 + 0.0062i		0.077
λ_{42}		62.0366 + 0.0062i		0.080
λ_{43}		65.4343 + 0.0062i		0.079
λ_{44}		68.8661 + 0.0062i		0.074
λ_{45}		72.1592 + 0.0062i		0.077
λ_{46}		75.6472 + 0.0062i		

Table 4.6: Undamped Euler-Benoulli beam model (continuation)

LIST OF REFERENCES

[1] D.J. Inman A. Erturk. Issues in mathematical modeling of piezoelectric energy harvesters. *Smart Materials and Structures*, Volume 17, 2008.

[2] Faruk Yildiz. Potential ambient energy-harvesting sources and techniques. *The Journal of Technology Studies*, Volume 35, 2009.

[3] D. J. Inman A. Erturk. An experimentally validated bimorph cantilever model for piezoelectric energy harvesting from base excitation. *Smart Materials and Structures*, Volume 18, 2009.

[4] *Britannica*, volume Dielectrics (physics). 2009.

[5] S.G. Kalashnikov. *Electricity*, volume Volume VI, pages 104–110. PHYS-MAT-LIT, 2003.

[6] Yates R.B. Williams C.B. Analysis of a micro-electric generator for microsystems. *Sensors and Actuators A: Physical*, Volume 52:8–11, March-April 1996.

[7] G. Despesse S. Boisseau and B. Ahmed Seddik. Electrostatic conversion for vibration energy harvesting. *Small-Scale Energy Harvesting*, 2012.

[8] D. J. Inman A. Erturk. *Piezoelectric Energy Harvesting*, pages 4–6. 2011.

[9] D. J. Inman A. Erturk. *Piezoelectric Energy Harvesting*, pages 54, 64. 2011.

[10] J.Ockendon P.Howell, G. Kozyreff. *Applied Solid Mechanics*, pages 152–153. 2009.

[11] J.Ockendon P.Howell, G. Kozyreff. *Applied Solid Mechanics*, pages 10–11. 2009.

[12] E. M. Purcell. *Berkeley Physics Courses: Electricity and Magnetism*, volume Volume II, chapter 3. 1965.

[13] D. J. Inman A. Erturk. *Piezoelectric Energy Harvesting*, page 94. 2011.

[14] E. M. Purcell. *Berkeley Physics Courses: Electricity and Magnetism*, volume Volume. II, page 23. 1965.

[15] D.C. Handscomb J.C. Mason. *Chebyshev polynomials*, pages 145–147. Chapman and Hall/CRC, 2003.

[16] Lloyd N. Berrut, Jean-Paul; Trefethen. Barycentric lagrange interpolation. *SIAM Review*, 46(3):pages 501–517, 2004.

APPENDIX A

Matlab code

A.1 Differentiation matrix

```
% This program computes the differentiation matrix
% The second, the third and fourth order differentiation matrices
% can be found by direct multiplication:
% D2=D*D;  D3=D*D*D;  D4=D*D*D*D
%This program run subroutine 'is_odd'
function [x,D] = dif_mat(N,LS)
%Chebyshev points expanded over [-LS,LS]
 x = LS*sin(pi*[ 1-N : 2 : N-1 ]'/(2*(N-1)));
%Treating N as index
   [N,m] = size(x);
   N = N-1;
%Initializing the derivatiation matrix
   D = zeros(N+1,N+1);
%Filling the element (1,1) and (N+1,N+1) of a matrix
   D(1,1) = (1 + 2*N^2) / 6;
   D(N+1,N+1) = -(1 + 2*N^2) / 6;
%Filling the diagonal
   for k=2:N
     D(k,k) = - x(k) / (2*(1-x(k)^2));
```

```
  end
% first row c0 = 2, ck = 1
  s = 1;
  for j=2:N+1
    D(1,j) = -(2*s) / (1*(x(1)-x(j)));
    s = -s;
  end
% first column ci = 1, ck = 2
  s = -1;
  for i=2:N+1,
    D(i,1) = s / (2*(x(i) - x(1)));
    s = -s;
  end
% other entries
  for i=2:N+1
    for j=2:N+1
      if i==j, continue, end
        % take care of (-1)^(j+i)
        s = is_odd(i-1+j-1);

        D(i,j) = s / (x(i) - x(j));
    end
  end
% adjusting the last row and the last column
D(1:N,N+1)=D(1:N,N+1)/2;
D(N+1,1:N)=D(N+1,1:N)*2;
end
```

```
%subroutine is_odd
% need this to figure out
% the sign of (-1)^(j+k)
function s = is_odd(x)
  if mod(x,2) == 0
    s = 1;
  else
    s = -1;
  end
end
```

A.2 Computation of eigenvalues of dynamics generator

```
% This program computes eigenvalues of dynamics generator
% This program uses subroutine dif_mat
% U(x,t) the unknown vector
% U(x,t)= [w(x,t), w'(x,t), v(t)]'
% where:
%       w(x,t) - transverse displacement of a beam,
%       v(t)   - voltage output,
%       t - time, 0< t < T ,
%       x - distance along unimorph energy harvester, 0< x <L.
% Input model constants
Y = 1 ;  % Young's modulus
m = 40 ;     % density of the flexible structure
Length = 200.0 ;   % length of the structure
C = 1.1e-5 ; % Capacitance
```

```
R = 6.0 ; % Resistance
kappa = -12.54 ;
Cs = 0 ; % Kevin-Voight damping (visco-elastic) coefficient
Ca = 0.01 ;  % air friction coefficient
I = 7.2 ;   % cross- section moment of inertia w.r.t. neutral axis
theta = 2 ; % opposing piezoelectric effect coefficient.
i = sqrt(-1) ;
% Scaled constants
E = Y*I/m ;
H = 1/(C*R) ;
G = Ca/m ;
%G = 0.0;
h = kappa/C ;
% The Chebyshev polynomials range from degrees n=0 : N-1.
N = input('Enter number of Chebyshev polynomials ') ;
% Get expanded Chebyshev collocation points
[xj,D] = dif_mat(N,Length/2);
D2=D*D;
D3=D*D*D;
D4=D*D*D*D;
% Assemble matrix bndry, whose kernel represents the boundary values.
r1 = zeros(1,N) ;
r1(1,1) = 1 ;
r2= zeros(1,N);
% 4 rows of bndry are 4 boundary conditions .
bndry = [      r1              r2        0 ;...
               D(1,:)          r2        0 ;...
```

```
                D2(N,:)          r2          0  ;...
                D3(N,:)          r2          0  ]  ;
B = null(bndry) ; % Orthonormal basis for ker(S)
%-------------------------------------------------------
% Assemble the matrix L = -i*(A^-1)*B
L = ...
    -i.*[ zeros(N)          eye(N)                  zeros(1,N)' ; ...
          -E.*D4(:,:)    -G.*eye(N)                zeros(1,N)' ; ...
           zeros(1,N)  -h*(D(N,:) -  D(1,:) )     -H          ] ;
%-------------------------------------------------------
% Compute B' * L * B
L_S = B' * L * B ;
% Compute eigenvalues of dynamics generator
el=eig(L_S);
 %-------------------------------------------------------
% Plot the eigenvalues of  B^t * L * B.
figure(1)
plot(el,'diamond','MarkerEdgeColor','k','MarkerFaceColor','b','MarkerSize',3)
ylim( [ -0.01  0.01 ] ) ;
xlim([ -0.01  0.01 ]) ;
xlabel('Real Axis') ;
ylabel('Imaginary Axis') ;
str(1) = {'Eigenvalues'}  ;
%str(2) = { [  ] } ;
%str(3) = { [ ] } ;
title(str,'FontSize',12) ;
grid on
```